In presenting the dissertation as a partial fulfillment of the requirements for an advanced degree from the Georgia Institute of Technology, I agree that the Library of the Institute shall make it available for inspection and circulation in accordance with its regulations governing materials of this type. I agree that permission to copy from, or to publish from, this dissertation may be granted by the professor under whose direction it was written, or, in his absence, by the Dean of the Graduate Division when such copying or publication is solely for scholarly purposes and does not involve potential financial gain. It is understood that any copying from, or publication of, this dissertation which involves potential financial gain will not be allowed without written permission.

3/17/65
b

LATERAL STABILITY OF STRUCTURAL TUBING SUBJECT TO PLASTIC MOMENT AND AXIAL LOAD

A THESIS

Presented to

the Faculty of the Graduate Division

by

Charles Richard Walters, Jr.

In Partial Fulfillment

of the Requirements for the Degree

Master of Science in Civil Engineering

Georgia Institute of Technology

September, 1967

LATERAL STABILITY OF STRUCTURAL TUBING

SUBJECT TO PLASTIC MOMENT AND AXIAL LOAD

Approved:

Chairman

Date approved by Chairman: Sept. 20, 1967

ACKNOWLEDGEMENTS

Through the aid of the Atlantic Steel Company, the efforts of Dr. F. W. Schutz, Jr., and the help of many others, this investigation was made possible. The writer is most grateful for the support of all who helped further this study. The Atlantic Steel Company, through its annual Atlantic Steel Fellowship, provided financial aid for a full graduate program in addition to sponsoring the thesis investigation. Additional financial assistance was given by Dr. C. R. Walters. The writer is deeply indebted to Dr. F. W. Schutz, Jr., faculty advisor, for his constant attention and advice, and for the initial program proposal. Mr. A. M. Franco, of Stein Steel, generously consented to fabricate the test frames. Much of the original work, organization of the program and procurement of the test sections was done by Mr. G. C. Lewis. Mr. R. R. Graham, of the United States Steel Company, was most generous in furnishing literature concerning recent work done on beam-columns of structural tubing. Final thanks go to the members of the reading committee, Dr. F. W. Schutz, Jr., Dr. A. B. Caseman, and Dr. P. H. Sanders, for their assistance and recommendations.

TABLE OF CONTENTS

LIST OF FIGURES

LIST OF FIGURES (continued)

LIST OF TABLES

LIST OF SYMBOLS

A - cross sectional area

b - width of cross section

c - distance from neutral axis to the extreme fiber of the cross section

d - depth of the cross section

e - eccentricity

f_{ult} - ultimate stress

f_y - yield stress

I - moment of inertia

I_{xx} - moment of inertia about the x - x axis

I_{yy} - moment of inertia about the y - y axis

l - length of beam or column

l_{eff} - effective length of column

M - moment

M_{exp} - experimentally recorded moment

M_o - reduced plastic moment

M_p - plastic moment

M_{12} - moment at joint no. 1 on member 1 - 2

P - axial load

P_{cr} - Euler critical buckling load

P_{ult} - ultimate axial load

P_y - plastic axial load; equal to A x f_y

LIST OF SYMBOLS (continued)

P_{24} - axial load permitted by formula 24 of the A. I. S. C. Code

r_{xx} - radius of gyration about the x - x axis

r_{yy} - radius of gyration about the y - y axis

t - wall thickness of section

δ_v - vertical deflection of the midspan plastic hinge of the simulated portal frame

δ_H - strong-axis deflection of the beam-column

ϵ - strain

ϵ_c - strain at the extreme fiber

ϵ_y - yield strain

θ - end rotation

θ_{12} - rotation at joint 1 for member 1 - 2

θ'_{12} - rotation of simply supported member 1 - 2 at joint 1 with the same loads as the original member before alteration of end conditions

ϕ - unit rotation

$\phi_{elas.}$ - elastic rotation

ω - uniform beam loading

$\Sigma\Delta$ - sum of readings of the upper and lower dial gages on the M - ϕ device

SUMMARY

The lateral bracing requirement for plastic design has proven to be a significant determent to its general application. Numerous braces are unsightly and expensive to fabricate. Restraining the compression flange of a beam-column in the plane of bending prevents failure by lateral-torsional buckling. Wide-flange sections are necessarily weak in torsion and lateral stiffness, and are extremely susceptible to this form of failure.

On the other hand, structural tubing has exceptionally good torsional resistance and lateral strength. Material near the neutral axis of a beam-column is loaded in compression, creating an efficient use of the entire cross section. There exists the possibility of significant savings in both material and fabrication costs through the use of structural tubing in plastically designed rigid frames.

The location of lateral bracing is a problem involving inelastic stability of a beam-column. The complete theoretical solution is not available for either wide-flange sections or structural tubing. Present plastic design procedures employ an empirical solution for use with wide-flange sections.

It was proposed that several beam-columns be tested to determine if there exists a practical range of loading for plastically designed frames of strucutral tubing without lateral bracing. The requirement was that adequate rotation of the plastic hinge occur before lateral-torsional buckling.

The test program indicates that there is a wide range of loads for which the plastic hinge rotation is more than adequate. Several portal frames are sketched which represent possible uses for those beam-columns which performed satisfactorily.

More extensive testing for the purpose of establishing design criteria for structural tubing without lateral bracing may prove to be a worthwhile project. A discussion is offered concerning the requirements of such an investigation. Work has been done at Lehigh University testing wide-flange sections to determine the upper limit of their applicability to plastic design without lateral bracing.

CHAPTER I

INTRODUCTION

The requirement for extensive lateral bracing of wide flange beam columns is one of the principal drawbacks of plastic design. There are several obvious reasons for this situation. Numerous light braces on the rafters and columns of building frames detract from what otherwise would be pleasing structural forms. The present trend toward more simple, massive steel structures is best seen in the newer steel bridges and public arenas. The move to simpler structures is at least partially caused by the high cost of fabrication. It is no longer economical to invest many man-hours in fabrication to save steel. The same principle applies for plastically designed one and two story structures. It is often more economical to use extra steel with elastic design than to incur the extra fabrication costs of lateral bracing for plastic design. For this reason, most metal building companies are converting from plastic design to computerized methods using elastic design. Finally, the current lateral bracing requirement, formula 26 (1),* is tedious to apply in the case of a building frame. It requires checking the ratio of end moments at numerous segments on the frame by a trial and

---

* Numbers in parentheses indicate literature cited in the "References" section of the Bibliography.

error basis, a laborious process if done accurately. In practice, lateral bracing is often located by guesswork once a designer has acquired some experience. All of these factors leave much to be desired in plastic design.

In some instances, structural tubing may be the answer to these problems. Its smooth appearance is more pleasing than the wide flange section. More importantly, its tubular shape has the high torsional resistance necessary to reduce or eliminate the need for lateral bracing. Thus, design and fabrication might be simplified. The fundamental objection to structural tubing is that the relatively large amount of web material is ineffective in bending. However, if combined axial load and moment act on the section, it becomes a most effective shape due to its high weak-axis column strength. Because the basic shape is a new one, it has not yet been fully investigated. Nevertheless, it is coming increasingly into favor with designers as its properties become better known.

Basic concepts of plastic design require that adequate rotation capacity of the "plastic hinge" be assured through a range in which the "plastic moment" is maintained. As a frame of the type to be encountered in plastic design is progressively loaded, sections under moment must rotate in order to offer a resisting moment. The rotation causes yielding of the section from the extremities toward the neutral axis. When yielding reaches its maximum depth, the resulting moment is known as the "plastic moment". Further rotation increases the resisting moment only through strain hardening, offering a relatively slight increase which is difficult to calculate accurately. Because

all hinges of a typical frame do not reach plastic moment simultaneously, a section is required to rotate at full resisting moment while other sections develop their "plastic moment". The rotation points are known as "plastic hinges". Normally, a rotation capacity of four to five times the elastic rotation is required.

As a section rotates at plastic moment, it tends to buckle out of the plane of bending due to a phenomenon known as "lateral-torsional buckling". Sections of low torsional and weak-axis bending resistance, e. g. wide flange sections, will tend to fail by lateral-torsional buckling if the compression flange is not braced. The problem is one of inelastic stability, and has been solved only for a wide flange section under one loading condition (2). The complete theoretical solution is not available for either open or closed sections, but work is being done in this direction. An empirical solution is commonly used for design of wide flange sections. While there is no similar formula available for structural tubing, its cross section is much more resistant to lateral buckling than the open, wide flange section. The tubular section is highly resistant to torsion, and the weak-axis bending resistance is relatively much greater than that of a comparable wide flange beam-column.

In light of the foregoing considerations, it would seem feasible that, without a theoretical solution, some conclusions might be drawn from testing the rotation capacity of typical frames without lateral bracing. Several parameters affect the lateral stability of a section:

1. The lateral support furnished by the end conditions.

2. The ratio of axial load to yield load, P/P_y, acting in conjunction with the plastic moment.
3. The slenderness ratio of the beam-column.
4. The geometry of the section tested.

Due to the practical limitations of a test program, it was feasible to work with only one cross section. Those sections with high depth to width, d/w, ratios are most subject to lateral-torsional buckling. Further details on the selection of a particular size tubing appear in "Description of Tests".

A portal frame was chosen as the type to be tested for two reasons. It is a most simple type of frame, and it would seem to be one of the best uses for structural tubing. The clean shape is ideally suited for framed openings. In each test a particular configuration and loading condition for a portal frame column is simulated by the proper ratio of axial load to end moment.

The purpose of the tests is to determine how the beam-columns perform under plastic moment and axial load without the benefit of lateral bracing. Does there exist a practical range of loading conditions in which structural tubing without lateral bracing might be used for plastic design?

CHAPTER II

DESCRIPTION OF TESTS

Selection of a Test Section

Sections with high d/w ratios are those most apt to fail by lateral-torsional buckling. A relatively narrow shape has low torsional resistance, and is subject to weak-axis buckling. Of the commonly produced sections, the highest d/w ratio occurs in the 6" x 2" x 3/16" section, in which d/w = 3. However, this ratio is produced only for the 6 inch deep section. The next highest ratio, d/w = 2, is produced for the 12, 8, 6, and 4 inch deep sections. In order that the test results might be applied to this more common section, the 6" x 3" x 3/16" structural tubing was selected. Mr. G. C. Lewis, who originally undertook the project, procured this material in sections 21 feet long.

Test Arrangement and Instrumentation

A particular portal frame configuration with a specific loading produces a predictable axial load and moment at the knee of the frame. Thus, it is only necessary to duplicate the moment and axial load to duplicate the column, or beam-column. Figs. 1 & 2 are pictures of the test setup with the beam-column in place. A twenty ton screw jack at the base of the frame was used to tension the cable while an electrical strain gage dynamometer in the system measured the cable load. Dial gages anchored to the fixed truss shown in Fig. 3 measured

deflections of the vertical member and were used to calculate end rotations at the joint. As near as practicable to the joint, a rotation measuring device, described in "Preliminary Testing", was affixed. By comparison with a previously established M - ϕ Curve, a measurement of the moment near the joint was obtained. Vertical deflections of the beam-column were measured at various stations along the length by reading scales attached to the beam from an engineer's level set off to the side of the test setup. Corrections for large deflections had to be made in these scale readings. An engineer's transit was set up at the foot of the column, though it does not appear in the figures. Three targets were affixed to the walls of the laboratory to establish a permanent vertical reference plane in the event the instrument was dislocated. At each station, horizontal scales were attached to the top and bottom of the beam. These can be seen from the end view of the test setup, Fig. 2. The difference in each pair of readings was used to calculate the twist at that station. A correction had to be applied at each station for a slight twist at the knee, which was not fixed. In this respect, the test conditions were more severe than those which might be encountered in an actual portal frame, which can be considered more nearly fixed against twisting than the test specimen. It should also be noted that it was necessary for the base plate to pivot with respect to the test fixture to handle large deflections. Because the jack was fixed to the base plate, the end conditions were not affected.

Test 1

Slenderness ratio affects the lateral buckling characteristic of a beam-column. As the length is increased, the column tends to buckle at lower axial load and the torsional restraint of the end conditions has less stabilizing influence on a central section under plastic moment. For Test 1 the maximum slenderness ratio allowed by the A. I. S. C. code in the plane of bending was chosen:

$$l / r_{xx} = 120$$
$$l = 252"$$

The axial load to be applied in combination with the plastic moment has to be a matter of guesswork for the first test. These factors were considered:

1. Euler weak-axis buckling load for a pinned-end column:

$$P_{cr} = (\pi^2 EI) / l^2$$
$$P_{cr} = 21.5 \text{ kips}$$

2. Formula 24 of the A. I. S. C. code for maximum axial load as limited by weak-axis bending stiffness:

$$P / P_y \leq 8700 / (l/r_{yy})^2 \text{ for } l / r_{yy} > 120$$
$$P = 29.4 \text{ kips}$$

Note that plastic design assumes that a load greater than the Euler weak axis buckling load for pinned ends can be supported. If an

l_{eff} = 0.85 l is used in place of the actual "l" in formula 24, the result is the same as the Euler formula. In effect formula 24 assumes that the column, due to partial fixity and lateral bracing, has an l_{eff} = 0.85. In the test case, there was some fixity at the column base but none at the top. The actual buckling load should be closer to the Euler load than the specification value.

Enough axial load had to be used to make the loading on the equivalent portal frame a practical one. For an axial load of approximately half the Euler buckling load, a practical span and loading could be achieved. At collapse, the end moment on the beam-column for uniform loading is the following:

$$M_p = wl^2 / 16$$

For a span length, l = 20 feet:

$$w = 16\ M_p / l^2$$

$$M_p = 290 \text{ in.-kip.}$$

$$l = 240 \text{ in.}$$

$$w = 80.5 \text{ \# / in.}$$

The axial load is then:

$$P = (1/2) \times w$$

$$P = 9.65 \text{ kip.}$$

and

$$P / P_{cr} = 45\%$$

$$P / P_y = 6.9\%$$

According to the A. I. S. C. code, formula 22, for a "Case 2" column, the full M_p is permitted. The loading satisfies all requirements except those for lateral bracing.

The eccentricity on the test specimen becomes:

$$e = M_p / P$$
$$e = 30.0 \text{ in.}$$

The vertical leg of the test specimen for Test 1 is 30.0 in. from the neutral axis of the column. The equivalent portal frame and loading for uniform and concentrated loads, is shown in Fig. 6.

Test 2

Having established the performance of the section at very high slenderness ratios, it was decided to reduce the length to one more typical of a column; $l / r_{xx} = 80$ was selected. The expressions for weak-axis buckling become:

1. Euler buckling load:

$$P_{cr} = (\pi^2 EI) / l^2$$
$$l = 172 \text{ in.}$$
$$P_{cr} = 46.0 \text{ kip.}$$

2. A. I. S. C. formula 24:

$$P = 8700 / (l/r_{xx})^2$$
$$P = 62.8 \text{ kip.}$$

For a portal frame 14 feet in height with a 10 foot span, the following loading produces a collapse mechanism:

$$M_p = w\, l^2 / 16$$

$$l = 120 \text{ in.}$$

$$M_p = 290 \text{ in.-kip.}$$

$$w = 322 \text{ \# / in.}$$

Total axial load becomes:

$$P = 19.3 \text{ kip.}$$

$$P / P_{cr} = 42\%$$

$$P / P_y = 13.9\%$$

Note that the axial load has been doubled, but that the ratio, P / P_{cr}, is held approximately constant.

The portal frame again is a practical one. If it were designed to support one half the uniform floor load for the end of a building with 20 foot bays, the ultimate floor load would be 386 psf., sufficient for the lighter warehouse loadings. The required eccentricity for the test specimen becomes:

$$e = M_p / P$$

$$e = 15.0 \text{ in.}$$

The equivalent portal frames with uniform and concentrated loads are shown in Fig. 7.

Test 3

After summarizing results of the first two tests, it was decided that the same slenderness as used in Test 2 would be maintained, but that the axial load would be increased for the next test. In so doing the similarity to practical portal frames was neglected in an effort to determine the effects of high axial loads. By altering the test fixture, replacing the 20 kip. dynamometer with a 50 kip. load cell located at the screw jack, it was possible to reach a P / P_y ratio of 0.3. From the interaction curve shown in Fig. 14, it is seen that there is a significant reduction in moment capacity at this high axial load. For the exact theoretical capacity of the section at a slenderness ratio of 80, an involved calculation is required. That calculation is discussed in "Theoretical Considerations", and a result of 206 in-kip. moment was predicted for an axial load of 0.3 P / P_y. The actual value for P is 41.76 kip.

The equivalent portal frame in this case is of little significance. However, for a column length of 172 in., the span is 40 in. for a uniform load of 2090 # / in.

At an axial load of 0.3 P / P_y or 41.76 kip., the ratio P / P_{cr} is high:

$$P / P_{cr} = 91.0\%$$

The ratio of axial load to ultimate load permitted by formula 24 becomes:

$$P / P_{24} = 66.5\%$$

The eccentricity for the test specimen becomes:

$$e = M_p / P$$

$$e = 4.92 \text{ in.}$$

The tension force for Test 3 was made to pass through a point 4.92 in. from the neutral axis of the beam-column.

CHAPTER III

PRELIMINARY TESTING

Due to inevitable production variations, the specified properties of any section are usually conservative with respect to the actual properties. To obtain accurate results, it is necessary to use the actual properties of the test specimens. The following preliminary tests were conducted to experimentally determine the section properties.

M - ϕ Test (Simple Beam Test)

The actual moment-rotation relation for the section was needed. Fig. 8 is a sketch of the test setup. On each side of the section are attached angles which extend the plane of the section above and below the beam. Dial gages are mounted to measure the change in slope of the plane sections. If the total change in the two dial readings, top and bottom, is $\Sigma\Delta$, then, by referring to Fig. 8 for the proper dimensions, the rotation is as follows:

$$\phi = \epsilon_c / c$$

$$\epsilon_c = \frac{\Sigma\Delta}{17} \times \frac{3}{17/2}$$

$$\epsilon_c = 0.0208\ \Sigma\Delta \text{ in./in.}$$

$$c = 3 \text{ in.}$$

$$\phi = 0.0069 \text{ rad. / in.}$$

Results of the M - ϕ test are shown in Table 1 and plotted in Fig. 9.

Coupon Tests

Three coupons were cut from the same section that was used for the M - ϕ test. All coupons were cut from locations which had not been highly stressed by the M - ϕ testing. A. S. T. M. specifications, (3), were followed with one exception. The test procedure dictated that the specified material thickness be used in calculations. In an effort to achieve more accuracy, the actual material thickness was measured by micrometer. This procedure gave a slightly different result than the standard method because the web and flange thicknesses varied somewhat. Table 2 shows the results of each coupon test and the values used for the actual properties. Fig. 10 is a stress-strain curve representation with pertinent values shown on the figure.

Cross Section Dimensions

Again, the section of beam used for the M - ϕ test was used to determine the dimensions of the cross section. Measurements were taken about one end of the five foot long beam. Equally spaced thickness measurements were made along web and flange, seven on each web, five on each flange. Table 3 shows these values. It is seen that the thickness varies considerably along web and flange.

Experimental Properties

Using the measured dimensions and the coupon test results, the experimentally determined design properties of the section have been calculated. Table 4 compares these to the specified properties.

The difference between the two is considerable. The experimentally determined properties have been used throughout this investigation.

It should be noted that the complete set of properties for the cross section were determined for one five foot section of the material selected at random from the stockpile. It was assumed that the remaining material had the same properties as that section. This assumption is not entirely accurate, but it should not introduce major errors into the results.

CHAPTER IV

THEORETICAL CONSIDERATIONS

Required Rotation Capacity

It was stated in the introduction that a plastic hinge rotation of four to five times the elastic rotation is usually considered adequate to develop all other hinges in a frame's collapse mechanism. Procedures for calculating the actual required rotation capacity are described in the Commentary on Plastic Design in Steel (4). The "plastic hinge method" has been used with the slope deflection equation to calculate the required hinge rotation. The procedure is as follows:

1. Draw the moment diagram for the collapse mechanism.
2. Assume the plastic hinges at the knees of the frame form first, and that continuity is preserved at the midspan hinge. Use the slope deflection equation to calculate the vertical deflection at the central hinge.
3. Assume the midspan hinge forms first, and that continuity is preserved at the knees. Use the slope deflection equations to calculate the deflection at the midspan hinge.
4. The calculation showing the largest deflection is the correct deflection and the first hinge formed is the one assumed in that calculation.

5. With the midspan deflection known, the slope deflection equation is applied again to the beam to obtain the rotation at the first hinge. The inelastic rotation is the rotation capacity required to establish the collapse mechanism.

This problem was solved for all three portal frames under the uniform load condition. Figs. 5 & 6 show the frames for the first two tests. The third frame was not shown in a figure because of its impractical dimensions, but its height was 172 inches with a 40 inch span. The solution was not attempted for the concentrated loading condition because the "plastic hinge method" results in large errors in curvature for sections under constant moment, as in the third point loading system.

Surprisingly, in all cases the first hinge to form was the midspan hinge. Moment distribution was carried out on all three frames to check that the midspan moment was greater than the joint moment. These solutions verified the "plastic hinge method", indicating that the first hinge actually does form at midspan.

Table 5 gives the values of the terms used in the slope deflection equation for each frame. Refer to that table for the form of the equation and to the adjacent sketch for notation. Apply the equation to span 2-1 to solve for θ_{21}, then to span 2-3, solving for δ_v.

With δ_v known, the equation is solved again to obtain θ_{32}. θ_{32} is the value of the inelastic rotation.

The elastic rotation was found from the experimental M - ϕ curve, Fig. 9, by extending the elastic and plastic portions of the

curve to their point of intersection at 6.48×10^{-4} rad. / in. It is common practice to assume that the plastic hinge spans approximately twice the depth of the section or, in this case, 12 inches. The elastic rotation becomes:

$$\phi_{elas.} = 6.48 \times 10^{-4} \times 12 = 0.00778 \text{ radians}$$

Finally, the ratio of the inelastic rotation to the elastic rotation is given in Table 5.

Note that in Table 5 the required rotation for Frame 3 is quite large. Due to the high axial load ratio, the slope deflection equation was inaccurate when applied to the column. Therefore the value of θ_{21} was taken directly from the numerical solution for the deflected shape as calculated in the following chapter, "Theoretical Considerations". The large required rotation is a result of the impractical geometry of the third frame. This should not be expected to occur in ordinary design problems.

Interaction Curve

For an axial load ratio, $P / P_y \leq 0.15$, there is no significant reduction in the moment carrying capacity of a beam-column. In the first two tests, P / P_y was less than that value; but for the third test, $P / P_y = 0.3$ was used. Thus, it became necessary to determine an interaction curve. For a slenderness ratio of zero, the calculation is made by simple plastic theory and is not difficult. However, for an $l / r_{xx} > 0$, the calculations become quite tedious.

For the case in which $l / r_{xx} = 0$, the Commentary on Plastic Design in Steel (4) derives the equations for the interaction curve of a wide flange section. The same ones apply to structural tubing sections. The basis for these equations is the assumption of a particular stress block which is divided into an axial load portion at the center, and moment resisting portions at the extremities. The interaction curve has been developed for the 6" x 3" x 3/16" structural tubing section. In Fig. 13 this curve is compared with that of a typical wide flange section. For $l / r_{xx} = 0$ it is seen that the tubular section has the greater curvature, indicating that relatively more web material exists for the tubular section. If the section were a solid rectangular one, the curve would be a quadrant of a circle.

In the case of a specific l / r_{xx} ratio greater than zero, the interaction curves for a typical wide flange section have been developed by Ketter, Kaminsky, Galambos, and Beedle of Lehigh University. Their results, which are widely used, show a plot of the various interaction

curves for slenderness ratios from 0 to 120 in increments of 20. Their derivation has been published in two reports of the Transactions of the American Society of Civil Engineers. (5, 6). Initially it is necessary to derive an M - P - ϕ curve for the particular section. To do this, a set of auxiliary curves is needed, from which, points of the M - P - ϕ plot can be directly determined. The auxiliary curves are developed from a set of nine equations (5). Equations for axial load, moments, and curvature are written for:

1. the elastic case
2. yielding into the flange
3. yielding into the web

The solutions are fitted together to form the auxiliary equations of Fig. 11. Points on the M - P - ϕ curve can be taken directly from Fig. 11 and plotted. This has been done for P / P_y = 0.1, 0.3, and 0.5 in Fig. 12. Values for P / P_y = 0.0 were taken from the experimental results.

The M - P - ϕ curve is then used to determine interaction curves for various slenderness ratios. Ketter and Galambos (6) outline the procedure, which is one of numerical integration. Initially, an axial load is selected, and numerical integration performed for an arbitrary selection of end moment. After several iterations, the process may converge to a particular deflected shape. In the numerical procedure, the M - P - ϕ curve is used to determine rotations which are beyond the linear range. A systematic process for accomplishing this unique type of numerical integration has been outlined in the above reference.

If the integration has converged to a particular deflected shape, a larger value of end moment is selected in combination with the same axial load. Another iteration is performed and the deflected shape determined. The process is continued until the iteration sequence diverges. The maximum moment for that axial load is the largest moment for which a deflected shape was obtained. This moment and axial load then establish one point on the interaction curve for a particular slenderness ratio. Because of the involved process, only four points were found to approximate the interaction curve for a slenderness ratio of 80. These four points involved approximately 45 repetitions of Newmark's procedure for computation of deflections (7).

A comparison is made in Fig. 13 between the interaction curves for the 6" x 3" x 3/16" structural tubing and the results for the typical wide flange section. As expected, the structural tubing developed more moment capacity at high P/P_y ratios than the wide-flange section for $l / r_{xx} = 0$. The same result might be expected for a slenderness ratio of 80; but, as Fig. 13 shows, the interaction curves are almost identical. The M - P - ϕ curve, Fig. 12, shows that, for every P / P_y ratio, the structural tubing has a higher moment carrying capacity than the 8 WF 31 wide-flange section used in the Commentary on Plastic Design in Steel, (4), Chapter 7, from which the typical wide-flange interaction curves were derived. Therefore, it should follow that the structural tubing interaction curve for $l / r_{xx} = 80$ have a larger moment capacity at the high P / P_y ratios than the wide-flange sections.

The explanation seems to lie in the terms of the ratio ϕ / ϕ_y:

$$\phi_y = e_y / c$$

"e_y" is a constant for the structural tubing and the wide-flange section. However, the distance to the extreme fiber, c, is different for the 8 WF 31 section and the six inch deep structural tubing. ϕ_y for the structural tubing is 33% greater than for the 8 WF 31 section. This difference could offset the more desirable M - P - ϕ curve for the structural tubing in the numerical integration procedure.

CHAPTER V

TEST RESULTS

Summary of Test Data

Tables 6, 7, & 8 show the pertinent test data in a condensed form for tests 1, 2, & 3 respectively. The recorded data has been converted to a useable form in these tables. The dynamometer readings for cable tension were converted to axial load in the column multiplied by the eccentricity to give end moment, columns 2 & 3. End moment varied linearly to zero at the column base. Axial load times deflection gave the second contribution to moment at each station. The largest total moment at any station for one reading was recorded as maximum moment, column 4. Twist calculations were recorded as described in "Description of Tests". A linear correction was applied to the twist measurements to compensate for the free end twisting at the top of the column. In each test twist readings were taken from the station recording the maximum twisting deformation. Weak-axis deflection was calculated as described in "Description of Tests" without correction. Strong-axis deflections, δ_H, had to be corrected for large deflections because the scales rotated out of vertical alignment due to geometry changes. End rotation was calculated using the dial gages attached to the truss shown in Fig. 3. The rotation measurement device was placed as near as possible to the knee in every test. Procedure for this calculation was described in "Preliminary Testing". Midspan

deflection, δ_v, of the portal frames was calculated in the section, "Load-Deflection Relationship", of this chapter to demonstrate that adequate load capacity was maintained during hinge rotation.

Interaction Curve

For each test, the maximum axial load and moment were plotted on the theoretical interaction curve, shown in Fig. 14. For tests 1 & 2, in which the axial load was less than 0.15 P_y, test results normally indicate greater than predicted capacity due to strain hardening. In the third test for $P / P_y = 0.30$, the rotation was inadequate to produce strain hardening. However, a result somewhat greater than the theoretical capacity was obtained. The only apparent explanation is that the cross section for the third test was larger than that tested in "Preliminary Testing" and/or the yield point was higher. In any case, the full capacity of the section was developed in every test without the benefit of lateral bracing.

Twist and Weak-Axis Deflection

In Figs. 15, 16, and 17, the maximum weak-axis deflection and the maximum twist are plotted on a common absicissa to determine which effect, if any, initiated a failure. Maximum twist and deflection were recorded as the maximum reading at any station. Normally, these values occurred at the same station. However, when the actual point of failure was located approximately midway between two stations, as in Test 3, Fig. 5, the greatest reading sometimes occurred at one station and then the other. This was the case in only two instances for Test 3,

and did not seem to effect the results.

In all three cases it can be seen from the figures that a radical change in the twist deformation occurred prior to the large lateral deflections. Each of these plots indicates the initiation of failure by lateral-torsional buckling. Though the actual twist is small compared to the lateral deflection, so small that in the early stages, it is not visibly noticeable, it is the instability to twist resistance that initiates the lateral, or weak-axis, deflection. This instability is noted on the figures as a radical deviation from the previous trend in twist deformation. In Fig. 15, the twist changes from a slight positive value to an increasingly negative one as the instability is reached. The negative twist indicates a counter-clockwise twist as viewed from the base of the column. The positive direction is clockwise. For weak axis deflection the positive direction was to the left as viewed from the base of the column. In Figs. 16 and 17, the twist is seen to reverse itself as the point of instability is reached. In each case, though, the significant point is that the twist instability initiated lateral buckling. This mode of failure is that of lateral-torsional buckling.

Moment-Rotation Curves

Figs. 18, 19, and 20 are plots of end moment and maximum moment versus end rotation. Maximum moment varied from end moment because, at large deflections, the axial load contributed additional moment to the beam-column. The method of calculation for these values has been described in the section, "Summary of Test Data" in this chapter. In

the initial stages of each test, maximum moment and end moment were the same because maximum moment occurred at the knee. As deflections became larger, the point of maximum moment moved away from the knee, and the difference between the two values occurred.

From Fig. 20 for Test 3, it is seen that the end moment never reached the value for maximum moment as in the first two cases. This was due to the high P / P_y ratio, and was predicted by the numerical integration procedure described in "Theoretical Considerations". In this case, the strong-axis deflection was so great that a larger moment was induced at an interior point on the beam-column than at the knee. Table 9 compares the predicted deflected shape and moments with those recorded in the third test. Deflections from reading #8, the last reading before failure of the specimen, were used. These values were increased by 19% so that the readings at station 4 would agree. It is seen that agreement is good between experimental and theoretical results. At station 2 the scale was not read because the cable had interfered with the line-of-sight at that station. The agreement is not as close between the two values recorded for moment at each station. The maximum difference of 6.5% could have been caused by variation of the cross section properties.

In Figs. 18 and 19 for Tests 1 and 2, the large differential between end moment and maximum moment at large rotations could easily be misinterpreted as a significant reduction in load carrying capacity. For this reason, the plots of axial load versus midspan deflection, δ_v, for a uniformly loaded portal frame, have been calculated and are

shown in Figs. 21, 22 and 23. From those figures, it is seen that the reduction in load carrying capacity at large deflections is not as serious as might be assumed from Figs. 18 and 19. This effect is discussed further in the section, "Load Deflection Relationship", of this chapter.

Rotation Capacity

In the chapter, "Theoretical Considerations", it was concluded that for the particular portal frames under consideration, the first hinge to form for a uniformly loaded frame was the hinge at midspan. Therefore, the hinges at the knees actually were only required to develop their plastic moment capacity without any rotation thereafter. Nevertheless, there are any number of practical portal frames in which the first hinge to form is at the knee. The alteration required for the simulated frame of these tests to form the first hinge at the knee would be to use a more flexible beam, stiffened in the vicinity of the knees. The relatively stiffer beam-columns would then carry more moment and force the hinges at the knees to form first. Therefore, the rotation capacity of a plastic hinge at the knee remains a problem of major significance.

Figs. 18 and 19 show a large rotation capacity under plastic moment. The end rotation has been plotted in degrees rather than radians in this case so that the magnitude of the rotation becomes apparent. In Test 1, Fig. 18, a rotation of approximately 6.75° is required to develop plastic moment. In Fig. 21 it is seen that essentially the same load is maintained through a midspan deflection,

δ_v, of 35 inches. This corresponds to a rotation of approximately 16.5°. Therefore, a plastic rotation of approximately 9.75° has occurred, or 0.17 rad. Using a calculated elastic rotation of 0.00778 rad., the plastic rotation was approximately twenty-two times the elastic rotation. The same calculation can be made for the second test. Since there is some reduction in load capacity before actual failure is reached, the specific amount of plastic hinge rotation is rather nebulous. Perhaps the most accurate statement to make in this case is that the rotation capacity for the first two tests was considerably greater than four to five times the elastic rotation normally considered adequate for the plastic hinge.

From Fig. 20, Test 3, it is obvious that the plastic hinge rotation was almost non-existent. Though the section did surpoass its theoretical maximum moment, lateral-torsional buckling occurred before any significant rotation. From this test, it must be concluded that lateral-torsional buckling does prevent hinge rotation at high axial load.

Load Deflection Relationship

Because of the apparent reduction in load carrying capacity indicated by the end moment reduction of Figs. 18, 19, and 20, it was necessary to plot the actual load capacity versus midspan deflection of the simulated portal frames. This was done for all three portal frames under uniform load conditions. These plots are shown in Figs. 21, 22, and 23.

The procedure used for obtaining the values of δ_v, which are

listed in Tables 6, 7, and 8, was similar to that described in "Theoretical Considerations". The "plastic hinge method" (4) was used, and the slope deflection equation:

$$\theta_{23} = \theta'_{23} + \frac{\delta_v}{l} + \frac{l}{3EI}\left(M_{23} + \frac{M_{32}}{2}\right)$$

The equation was applied to section 2-3 of the beam sketched in Fig. 21. Rather than use the theoretical θ_{23}, the actual measured value, from Tables 6, 7, and 8 was used. The end rotation for a simply supported beam with the same loading is given by:

$$\theta'_{23} = \frac{wl^3}{24EI}$$

as in "Theoretical Considerations", the value M_{2-3} was the actual recorded end moment. In all cases, after the plastic hinge had formed, M_{32} was set equal to the value of M_p. A tabular solution was made for each reading. The results are shown in column 10 of Tables 6, 7, and 8, and plotted in Figs. 21, 22, and 23.

It is seen in Fig. 21, that the actual reduction in load capacity is insignificant throughout most of the deflection. In Fig. 22, the same is true. The scales are not held constant for the two figures in order that the elastic portion of the curves can be held at approximately the same slope. In Fig. 23, the load drops off sharply with vertical deflection, but in this case it has been determined that lateral-torsional buckling failure had previously occurred. Therefore, in no case tested was the reduction in load capacity due to geometry change a means for concern.

Local Buckling

It has been noted that initially all three failures were by lateral-torsional buckling. When this type failure occurs, the lateral deflection increases rapidly with essentially no increase in load. If this deflection is carried far enough, the section will warp as shown in Figs. 4 and 5. This phenomenon is known as local buckling.

Fig. 4 is a picture of local buckling which occurred in Test 2. It should be noted that both the web and flange show signs of this type failure. The lateral deflection of 5.02 in. was quite large. The strong-axis deflection of 11.48 in. was also large. In Fig. 19, the sharp dropoff in maximum moment is due to local buckling.

In contrast, Test 1 was stopped just before local buckling occurred. In Fig. 15, it is seen that the column had failed by lateral-torsional buckling and that lateral deflection was rapidly increasing. However, the maximum travel of the screw jack was reached at a lateral deflection of 2.75 inches, and a strong-axis deflection of 13.4 inches. No dropoff in maximum moment was observed, Fig. 18, and no signs of local buckling were seen.

In Test 3, local buckling occurred when a large lateral deflection was reached, with relatively little strong-axis deflection. The test was stopped at a lateral deflection of 3.95" and strong-axis deflection of 3.4" after local buckling had occurred. Fig. 5 shows the local

buckling for this test. It should again be noted that both the flange and web buckled locally.

Axial Load versus Maximum Strong-Axis Deflection

In Fig. 24, axial load versus maximum strong-axis deflection has been plotted for all three tests. As shown on the adjacent sketch, that deflection is the δ_H of the beam-column. As might be expected, these curves are very similar to those of Figs. 21, 22, and 23 where δ_v versus axial load was plotted.

End Moment Check

Originally, the rotation measuring device was intended to be placed at the section of maximum moment for the purpose of measuring that moment. However, in Tests 1 and 2, it was seen that the plastic hinge originally formed at the knee and moved toward the column base until failure finally occurred near the quarter point. This moment was due to the large deflections which contributed to the moment. Therefore, the M - ϕ device was placed as close as possible to the knee of the beam-column because the exact location of the failure could not be predetermined. In the third test it was located in the same place, to be used as a check on the end moment. Figs. 25, 26, and 27 show the correlation between end moment as measured by the dynamometer and that measured by the M - ϕ device. It is seen that the agreement is fair. The more direct method, the dynamometer and load cell, were used as the correct readings.

CHAPTER VI

DISCUSSION AND CONCLUSIONS

The overall performance of the structural tubing was surprisingly good. The tests indicate that there exists a large practical range in which beam-columns of structural tubing may be used for plastic design without any lateral bracing. These sections are extremely economical when loaded in compression and bending, both in material savings and simplicity of fabrication.

Table 10 is intended for use in comparing the significant parameters of the three tests. Note that the "P_{cr}" in column 4 is the Euler weak-axis buckling load for a pinned end member. The test rig actually imparted a small degree of fixity to the column base, so that the actual buckling load should have been somewhat larger than "P_{cr}". In column 5, the P / P_y is that maximum axial load as limited by the weak-axis buckling strength according to formula 24 (1). Formula 24 permits an axial load equal to the buckling load for an l_{EFF} = 0.85. Evidently it has been assumed that lateral bracing requirements reduce the l_{EFF} of a column to less than 0.85 L. In column 5 the "M_o / M_p" ratio is that calculated for a "Case 11" column, formula 22 (1). The "ult." subscript indicates the maximum load recorded in the tests.

Slenderness Ratio

For both the strong and the weak axis, slenderness ratios were

not a limiting factor if used with normal axial loads. The maximum permissible ratios, $l / r_{xx} = 120$ in the plane of bending, $l / r_{yy} = 203$ perpendicular to the plane of bending, were tested simultaneously and found to exhibit much more than adequate rotational capacity. The axial load, $P_{ult} / P_y = 6.8\%$, was large enough to be in the practical range for a beam-column. For example, the loading combination is that which would be imposed on the beam-column in the portal frame of Fig. 6.

Axial Load

High axial load did reduce the rotational capacity of the beam-column. For an $l / r_{xx} = 80$, and $P / P_y = 31.9\%$ plastic hinge rotation was negligible. However, for $P / P_y = 13.8\%$, more than adequate rotation developed. Again, this axial load is sufficient to support a highly loaded portal frame, Fig. 7.

Cross Section Geometry

As the ratio of r_{xx} / r_{yy} decreases, that is as the section approaches a square shape, the resistance to torsion and to weak-axis buckling is increased. Therefore, any section with an r_{xx} / r_{yy} ratio less than that used in the tests should perform as well or better than the test section.

CHAPTER VII

RECOMMENDATIONS

Until an accurate theoretical or empirical solution to the problem of inelastic rotation in beam-columns of structural tubing is devised, it may prove advantageous to formulate an approximate solution as a design method. It appears that such an approximation might be accomplished using a reasonable number of tests. The problem is to eliminate as many variables as possible.

Wall thickness is one variable which has not yet been mentioned. For each nominal size of tubing, there are several available thicknesses. Tests could be conducted on each extreme of thickness for several nominal sizes to determine which extreme, if any, consistently gave the most conservative results. Since the thickness variations are minor compared to the overall geometry of the section, it should be expected that results expressed for one thickness, axial load in terms of P / P_y for example, would be fairly accurate for other thicknesses.

The ratio, r_{xx} / r_{yy} is another variable which has a more pronounced effect on the performance of the section, as discussed in the "Conclusions". Fortunately, there are only a few major variations in the r_{xx} / r_{yy} ratio. A depth to width ratio, $d / w = 2.0$, was tested. All sections with $d / w = 2.0$ have approximately the same r_{xx} / r_{yy} ratio.

Square sections, d / w = 1.0, should also be tested, and possibly a section with d / w = 1.5, such as a 6" x 4" section.

The loading conditions, such as the presence of one or two end moments, producing single or double curvature, also must be recognized as variables. Results would have to be separated into Case 1, 2, or 3 columns, as in the A. I. S. C. Code.

Ultimately, the slenderness and axial load ratios become the only remaining major variables. Tests might be made using slenderness ratios in increments of 20 to a limit of 120, to determine the maximum P / P_y ratio that permits adequate rotation capacity. For example, for the three tests conducted, it might be said that, for a Case 2 column with d / w ≤ 2.0, adequate rotation capacity exists without lateral bracing for:

1. $l / r_{xx} \leq 120$; $P / P_y \leq 7\%$
2. $l / r_{xx} \leq 80$; $P / P_y \leq 15\%$

It should not be expected that this problem will be accurately solved by experimentation, because there are too many variables involved. However, if an acceptable theoretical solution is not forthcoming in the near future, a test procedure similar to this one may prove to be a worthwhile project.

In the course of this investigation, it was necessary to approximate the interaction curve for structural tubing. A comparison of the curves for wide-flange sections versus the tubing, Fig. 13, shows that substantially more strength at higher axial load ratios is

predicted for the latter. This situation can be used to advantage if plastic design methods are applied to structural tubing as previously discussed. When the interaction curves for wide-flange sections were derived (6), the hand calculations were time consuming, but necessary. Using a computer, the same calculations could be made with relatively little effort. The curves for structural tubing could then be translated into column formulas similar to those now written into the A. I. S. C. Code for Case 1, 2, and 3 columns. Material savings based on new design formulas should be substantial and well worth the effort used in their derivation.

APPENDIX A

APPENDIX A

It was suggested by Dr. P. H. Sanders, of the reading committee that a discussion of the relative economy of structural tubing versus wide-flange sections be included. The following is a cost comparison of equivalent designs using structural tubing in one case and wide-flange sections in the other. The prices quoted within were given by the Bethlehem Steel Corporation for the required sections cut to the proper lengths, and shipped to Atlanta, Georgia. For the wide-flange designs, an additional thirty percent was added to the cost of the steel to cover the cost of the lateral bracing in-place.

For the structural tubing design, the specified properties of the section were used in order to derive a collapse load for each frame. For the frames of the second and third test, the theoretical interaction curve for $l / r_{xx} = 80$ was used to determine the reduced moment capacity under combined loading. This procedure gave the collapse load which would be derived using normal design methods and did not incorporate any of the extra capacity found by experimental methods.

The previously derived loads were then used in the design of wide-flange columns for the three portal frames. In this case, the A. I. S. C. plastic design formula number 22 for a Case 2 column was used. For all three portal frams a 6B12 section was found to be the lightest adequate section. The same section was used for the horizontal member. Though the 10.6 lb./ft. weight of the structural

tubing section compares favorably with the 12 lb./ft. weight of the wide-flange section, the difference occurred only because there was no wide-flange section which was perfectly suited for the particular application. The 6B12 section was somewhat heavier than absolutely necessary. Bethlehem Steel Corporation quoted a price of $17.05 per hundred pounds of structural tubing cut to size and shipped to Atlanta, Georgia, and $9.50 per hundred pounds of wide-flange section, cut and shipped. For the portal frame of Test 1, the price per frame for the steel alone was $111.92 for the structural tubing, and $70.69 for the wide-flange sections. To this price, an extra thirty percent was added to the wide-flange columns to cover the in-place cost of lateral bracing. The following are the steel and lateral bracing costs for the columns used in the portal frames of Test 1:

Structural Tubing	$111.92
Wide-Flange Section	$ 91.90
Percent Difference	22%

The cost of steel, using the structural tubing design, is 22% more than for the steel and lateral bracing in-place, using wide-flange sections. This cost differential would have to be balanced against the cleaner appearance of the structural tubing without the lateral bracing.

APPENDIX B

FIGURES

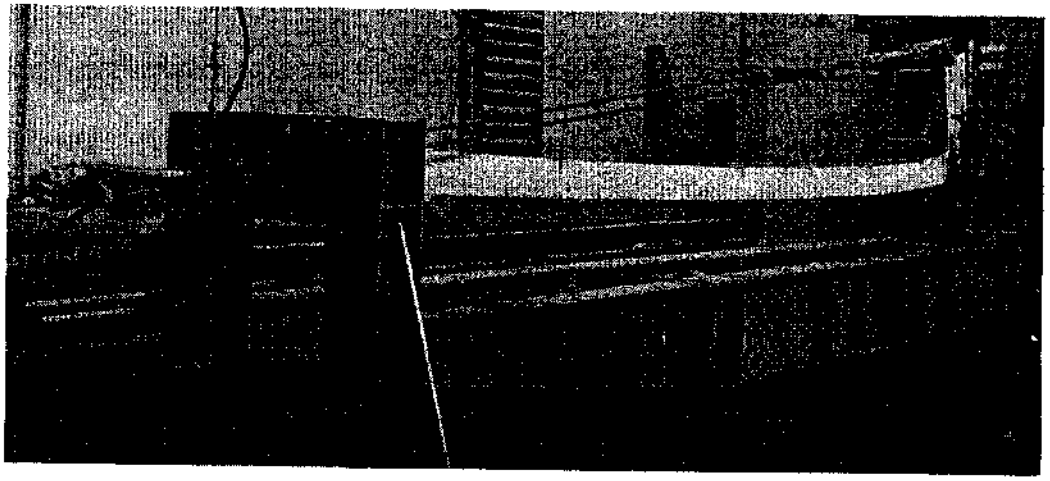

Figure 1. View of Typical Test Arrangement.

Figure 2. End View of Typical Test Arrangement Showing Scales for Measurement of Lateral Deflection.

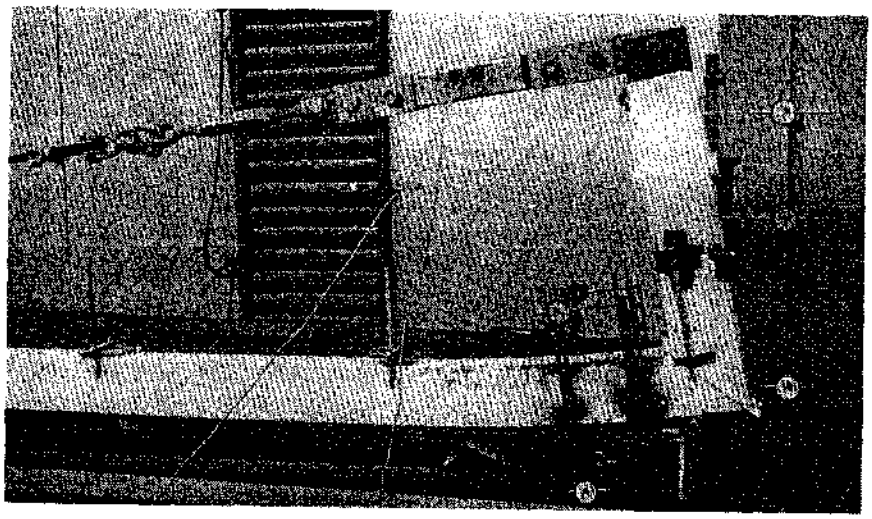

Figure 3. View of M - Device & End Rotation Instrumentation.

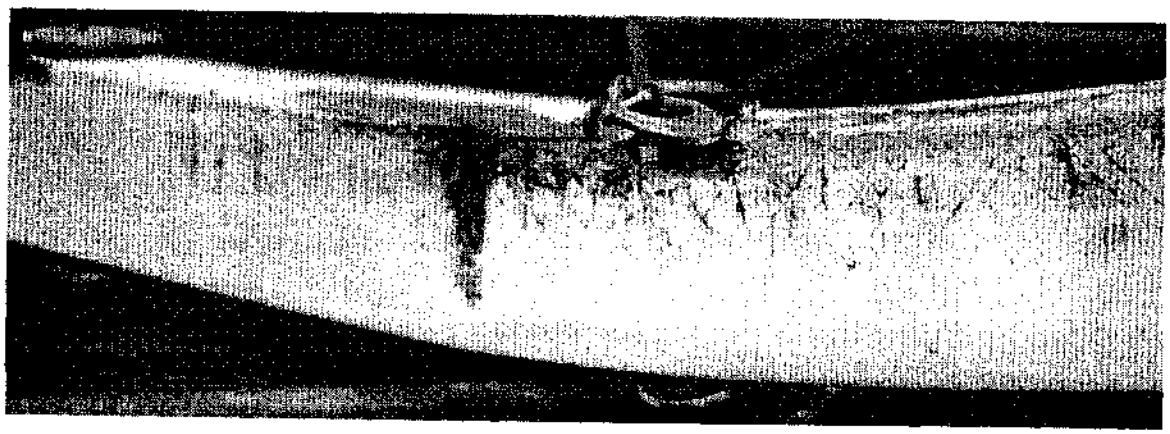

Figure 4. Test 2: View of Local Buckling.

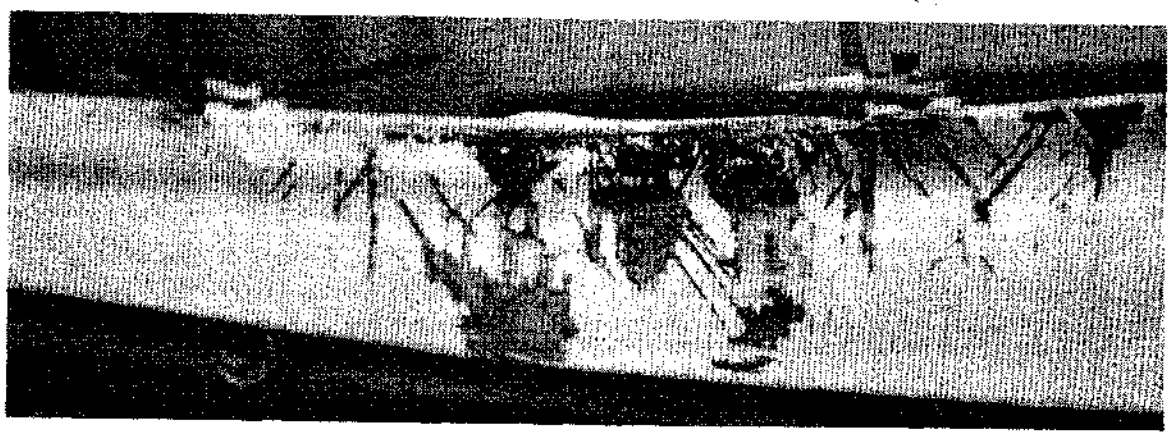

Figure 5. Test 3: View of Local Buckling.

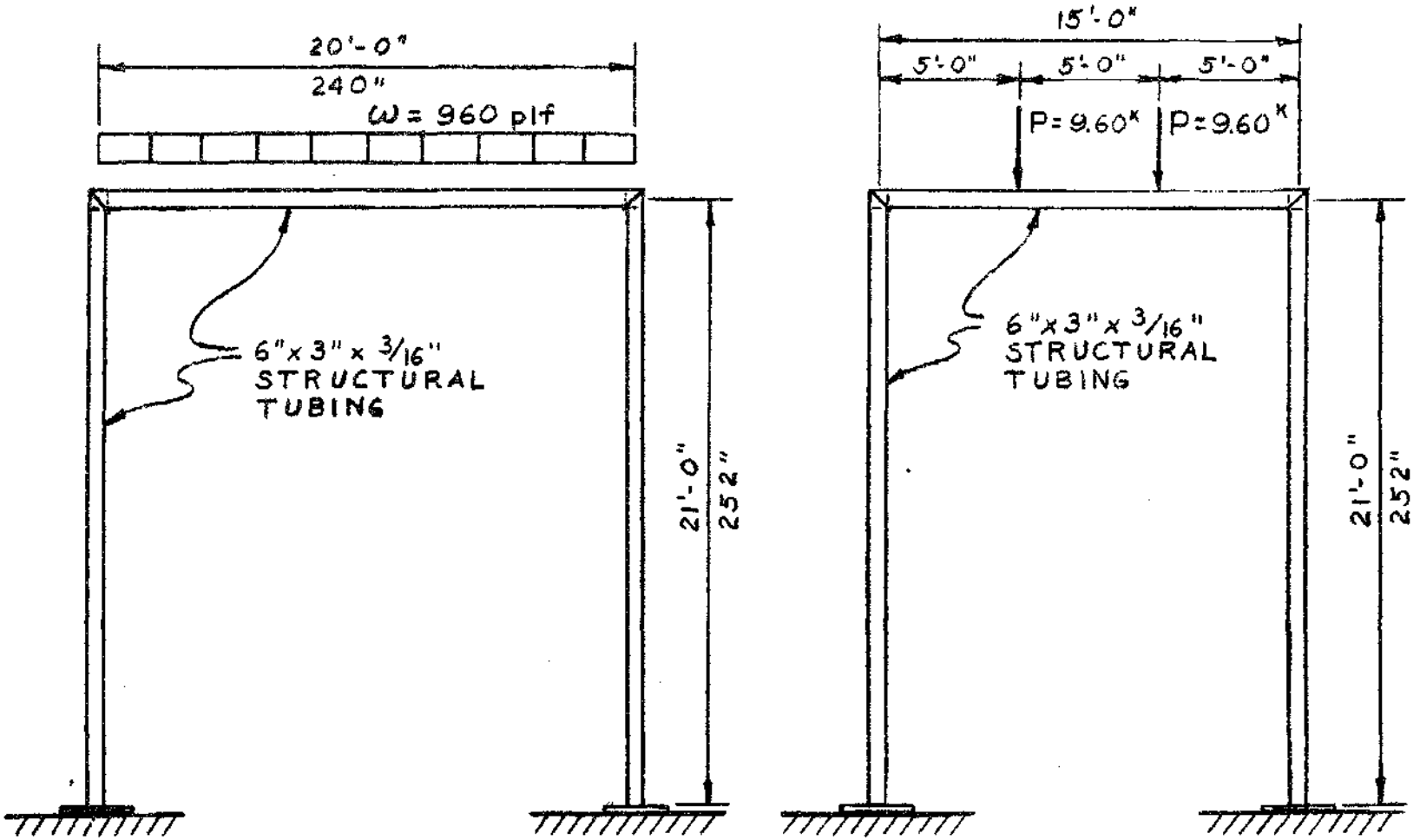

A. UNIFORM LOAD

B. CONCENTRATED LOAD AT 1/3 POINTS

Figure 6. Test 1 - Simulated Portal Frame

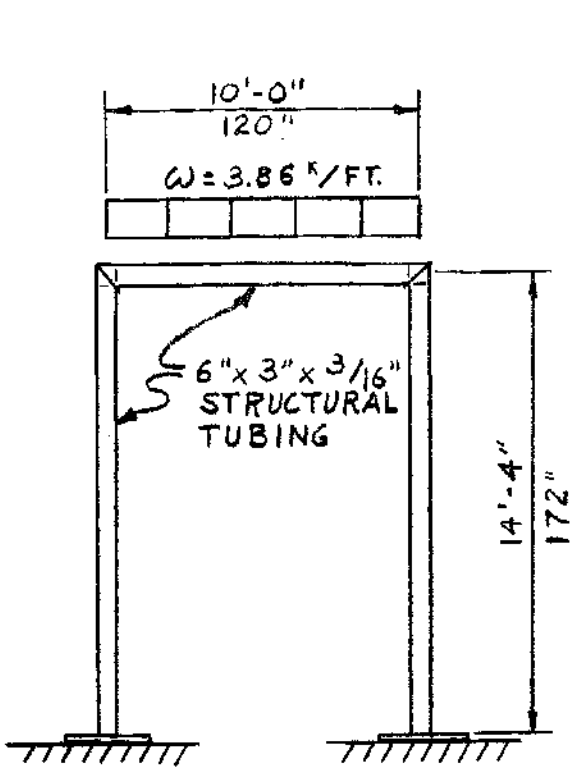

A. Uniform Load

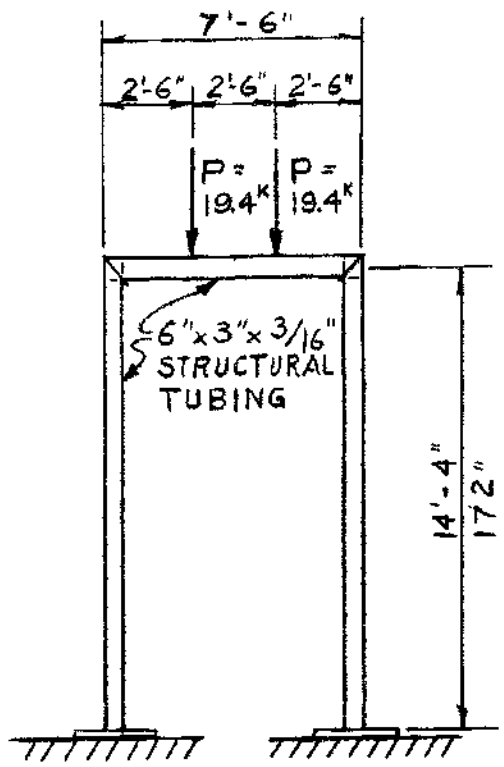

B. Concentrated Load At 1/3 Points

Figure 7. Test 2 - Simulated Portal Frames

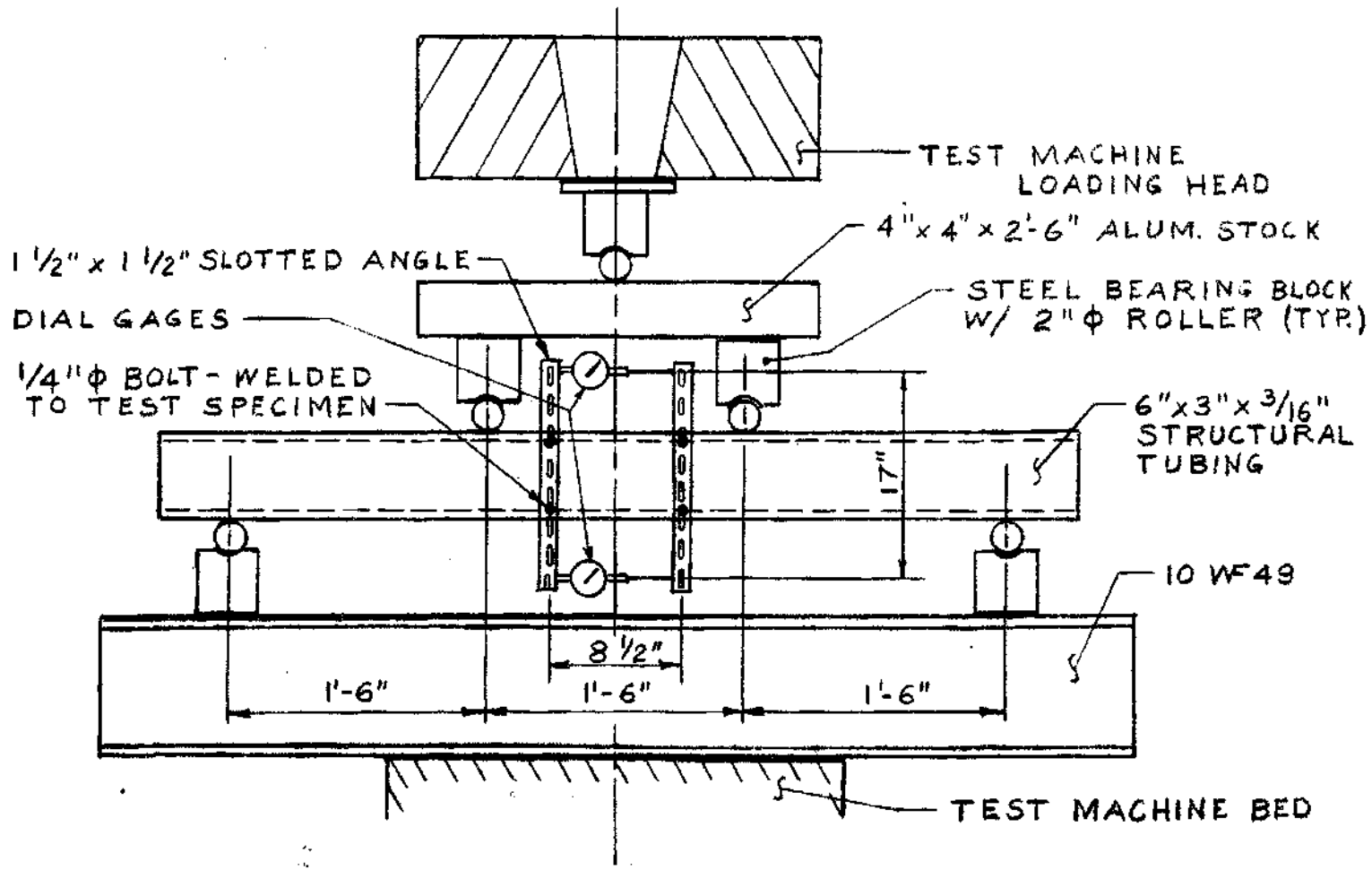

Figure 8. Sketch of M - Φ Test Arrangement

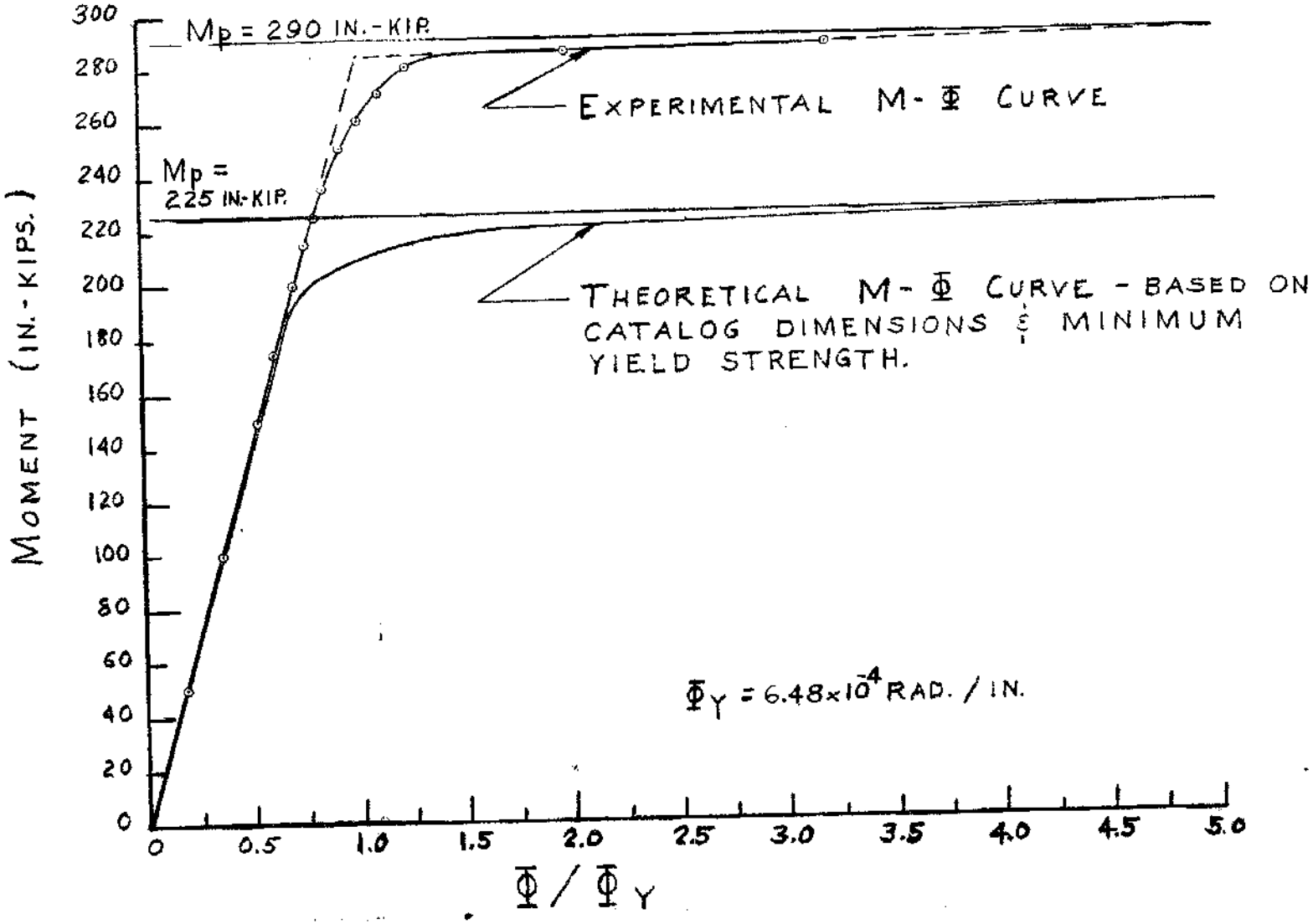

Figure 9. Theoretical & Experimental M - ϕ Curves

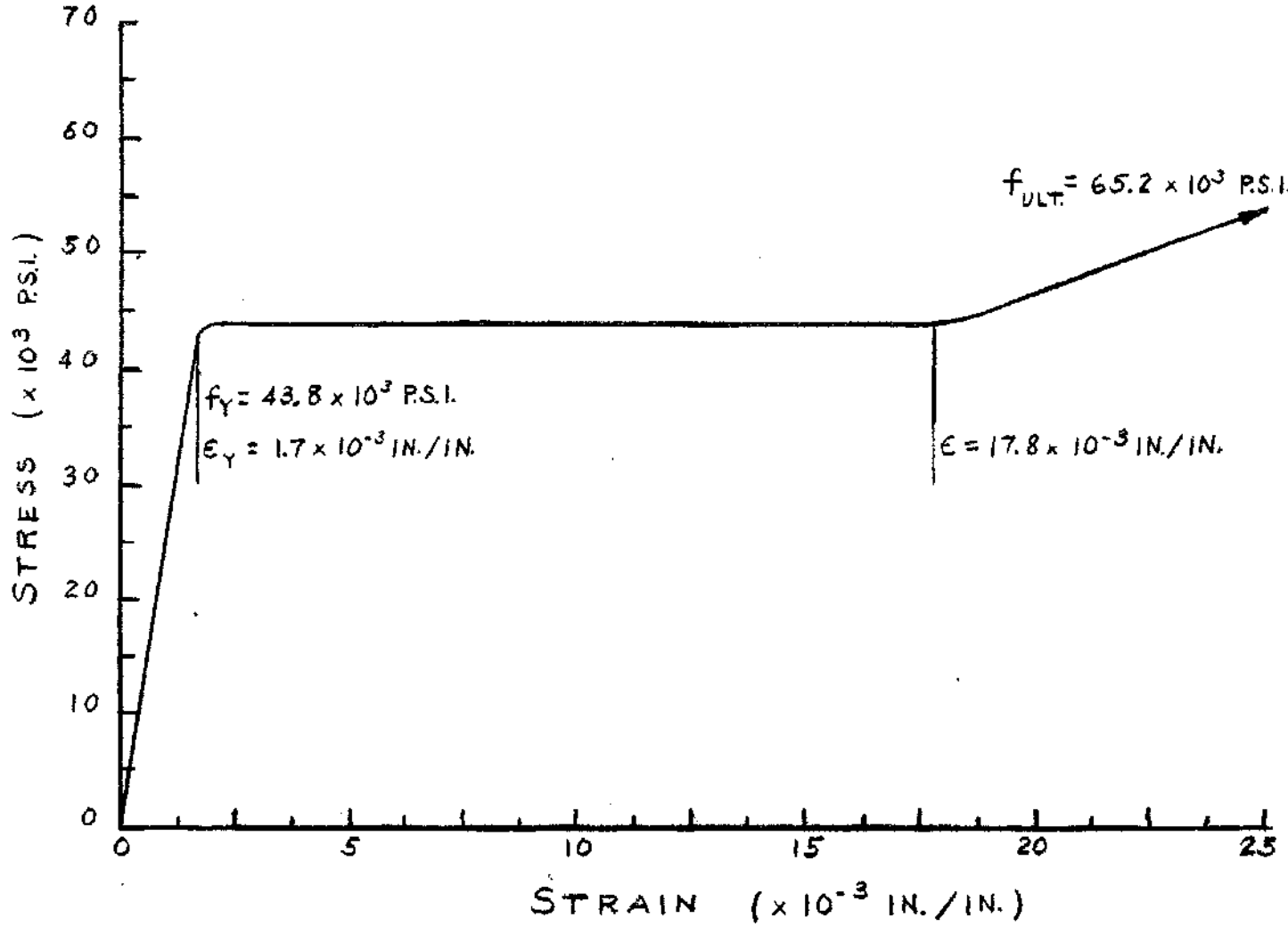

Figure 10. Experimental Stress - Strain Curve

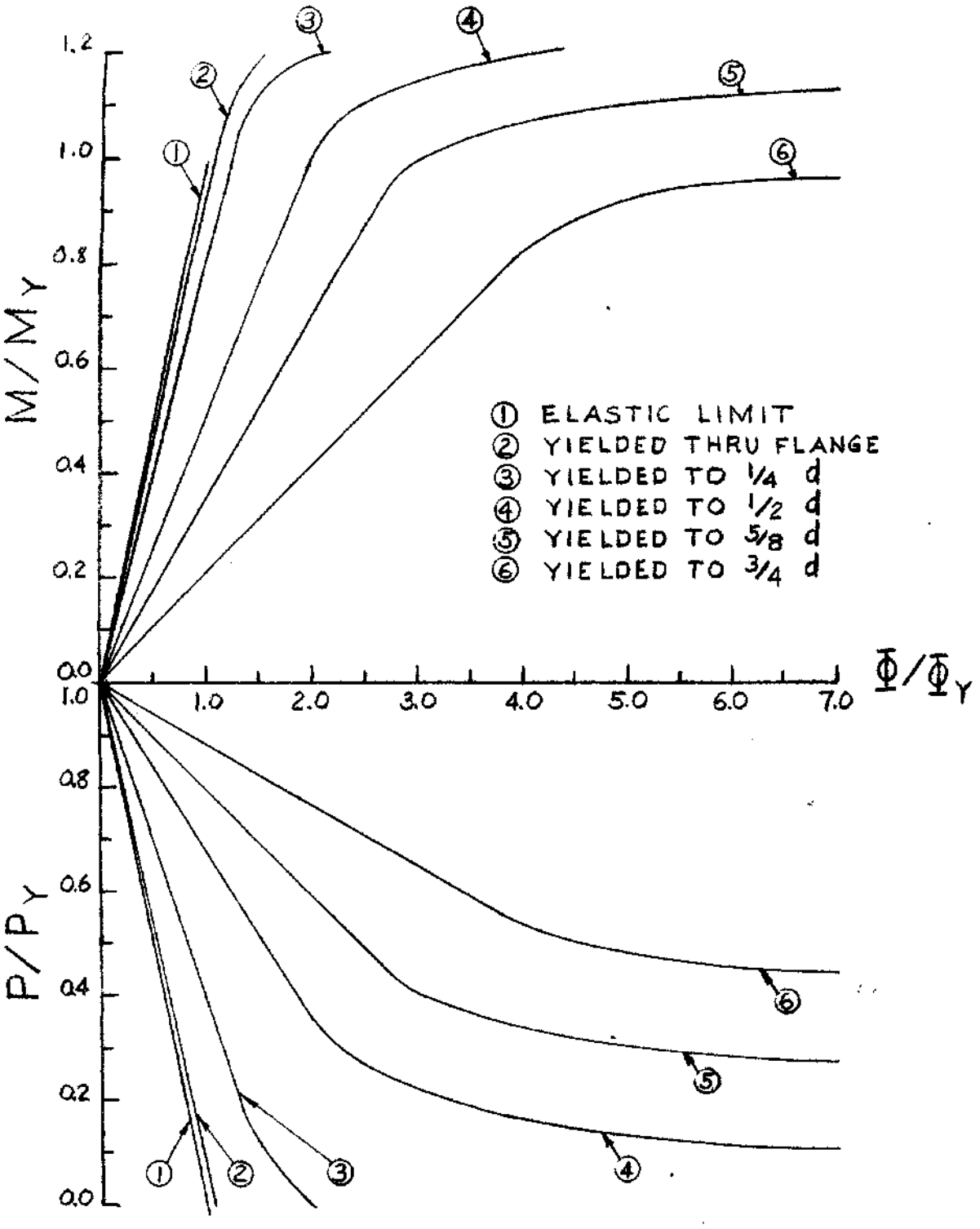

Figure 11. Auxillary M - P - Φ Curves

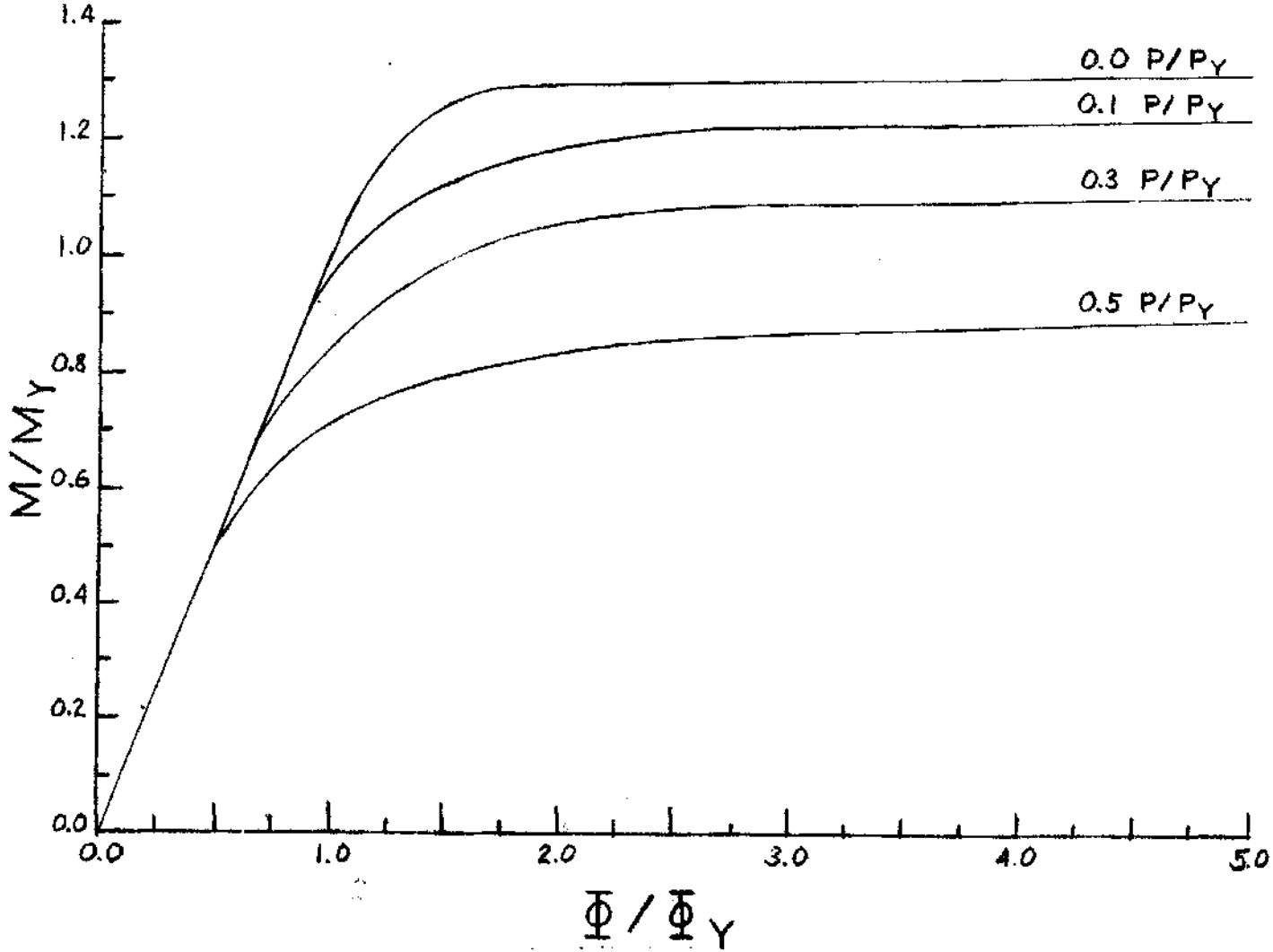

Figure 12. M - P - Φ Curves

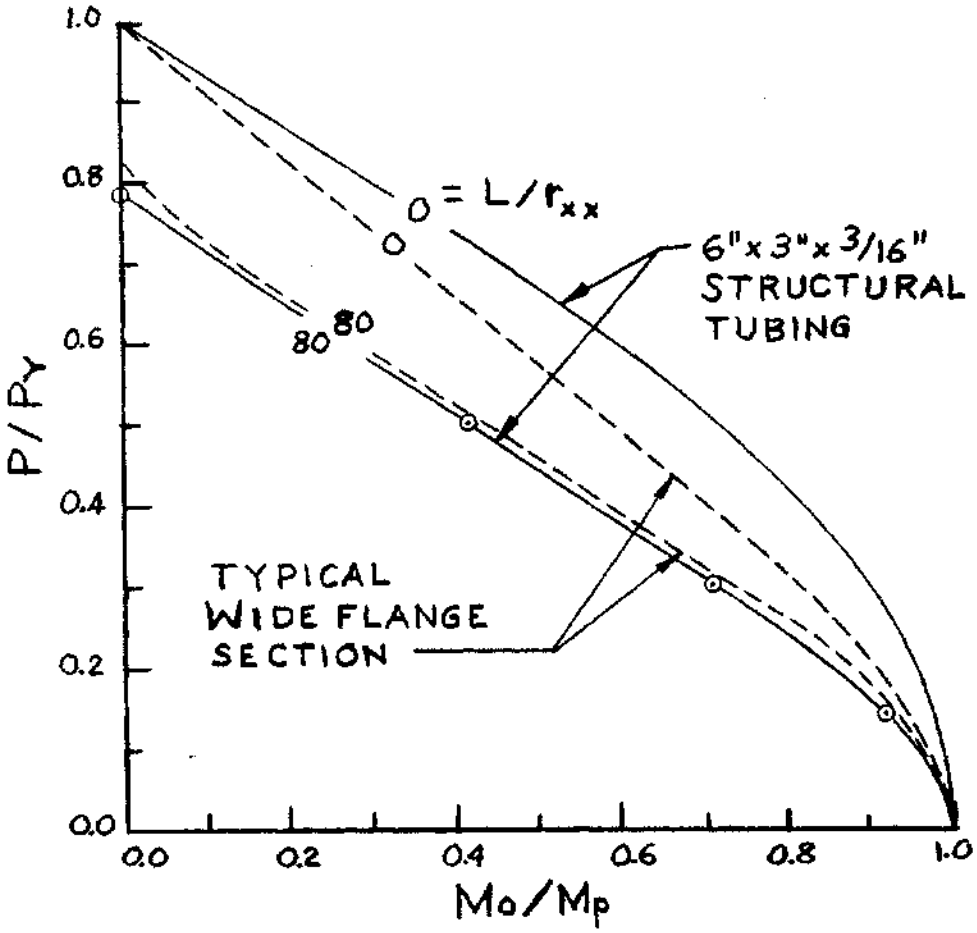

Figure 13. Comparison of Structural Tubing and Wide-Flange Interaction Curves

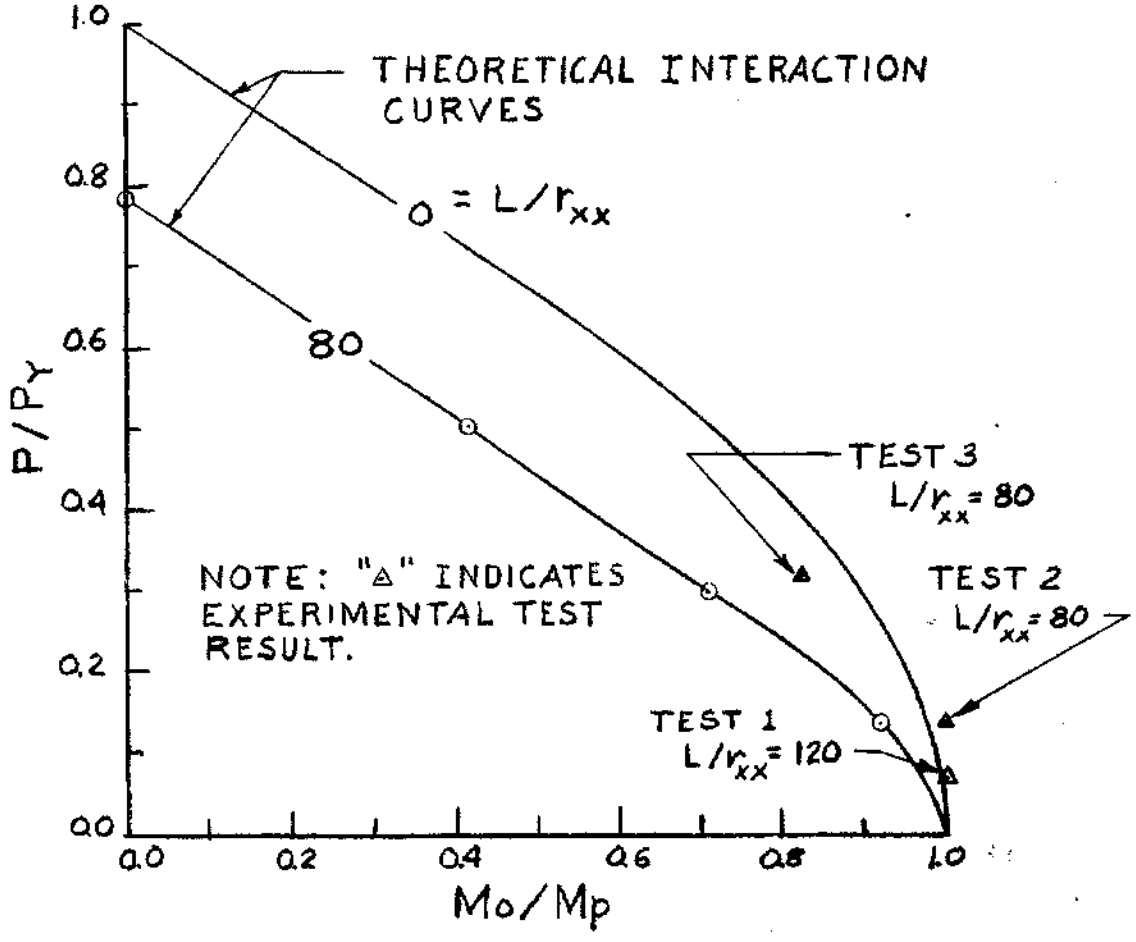

Figure 14. Comparison of Test Results with Theoretical Interaction Curves

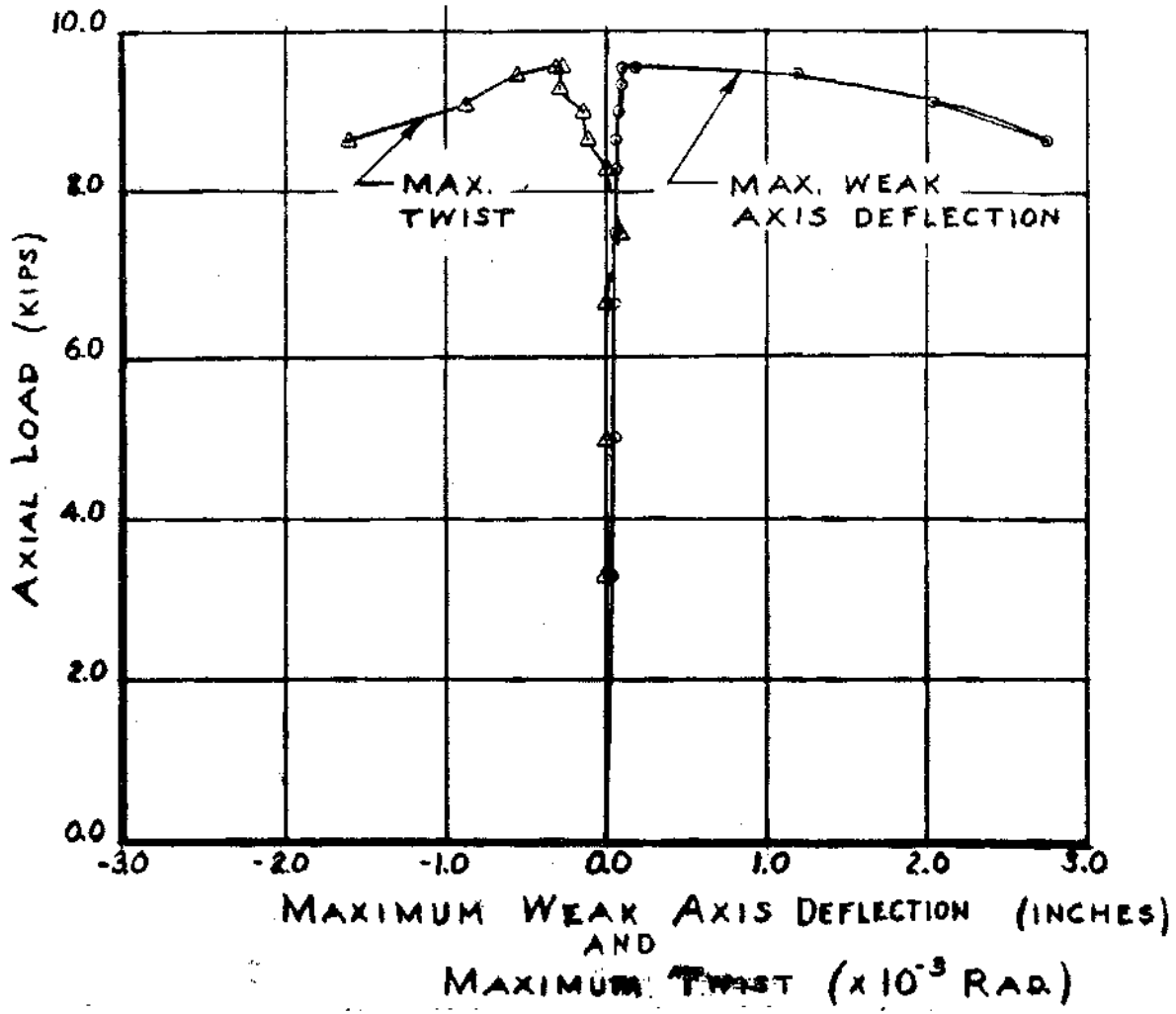

Figure 15. Test 1 : Twist and Weak Axis Deflection Curves

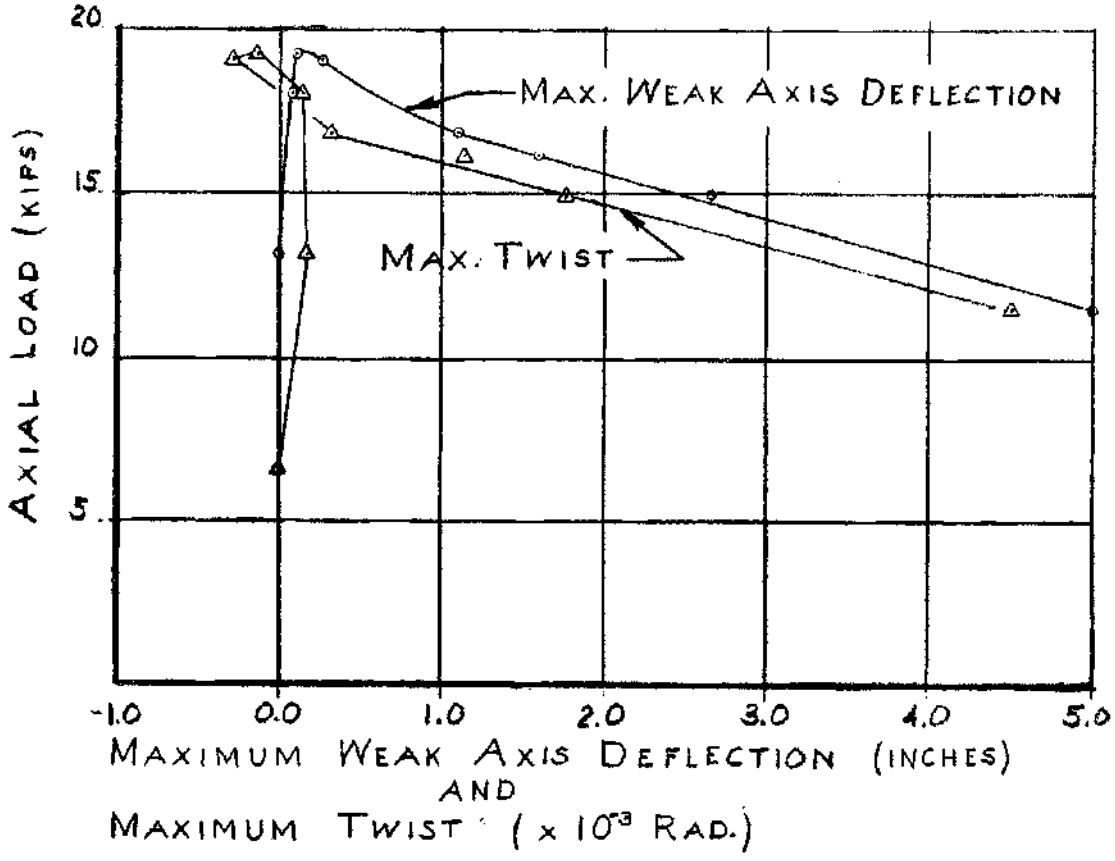

Figure 16. Test 2 : Twist and Weak Axis Deflection Curves

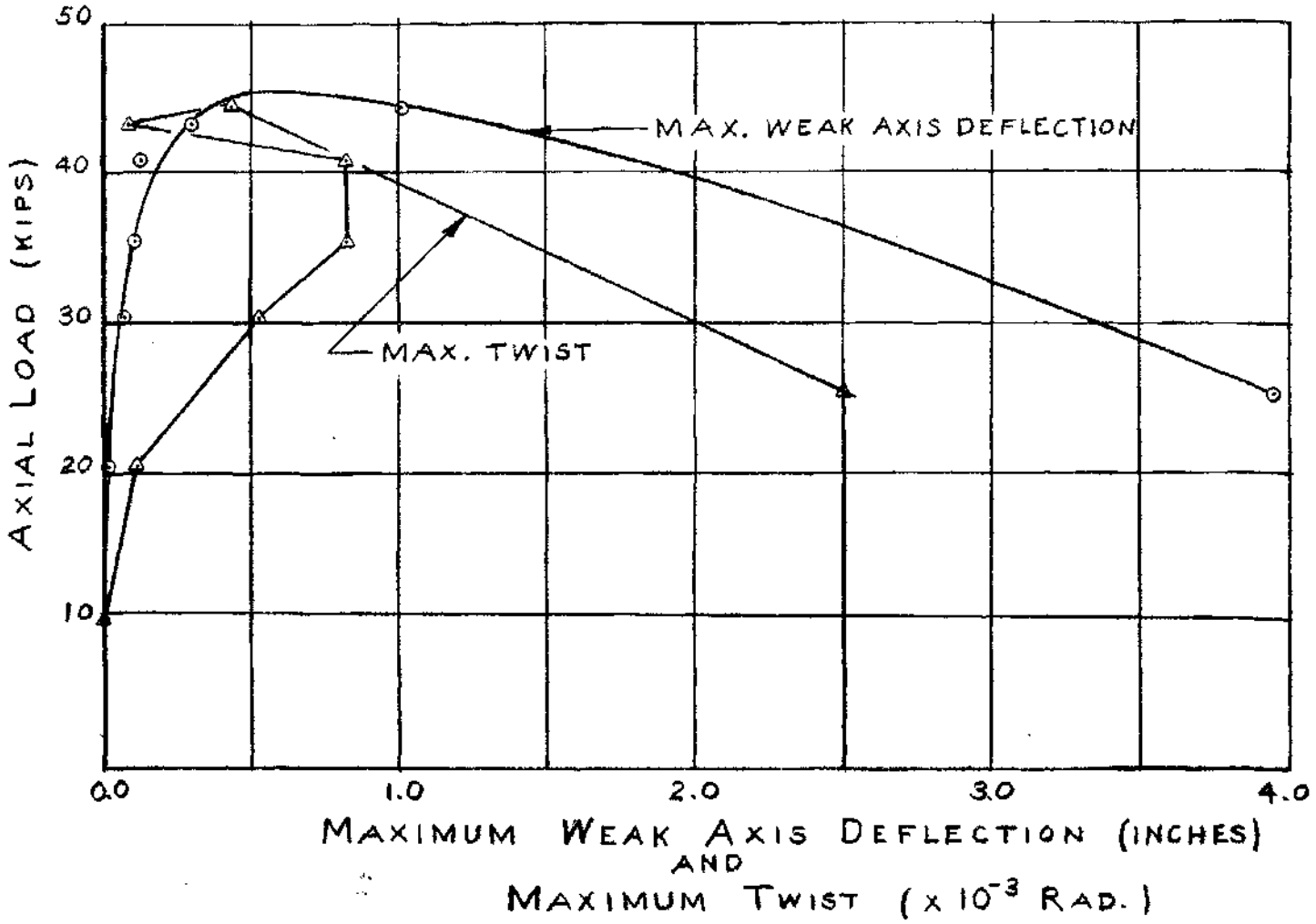

Figure 17. Test 3 : Twist and Weak Axis Deflection Curves

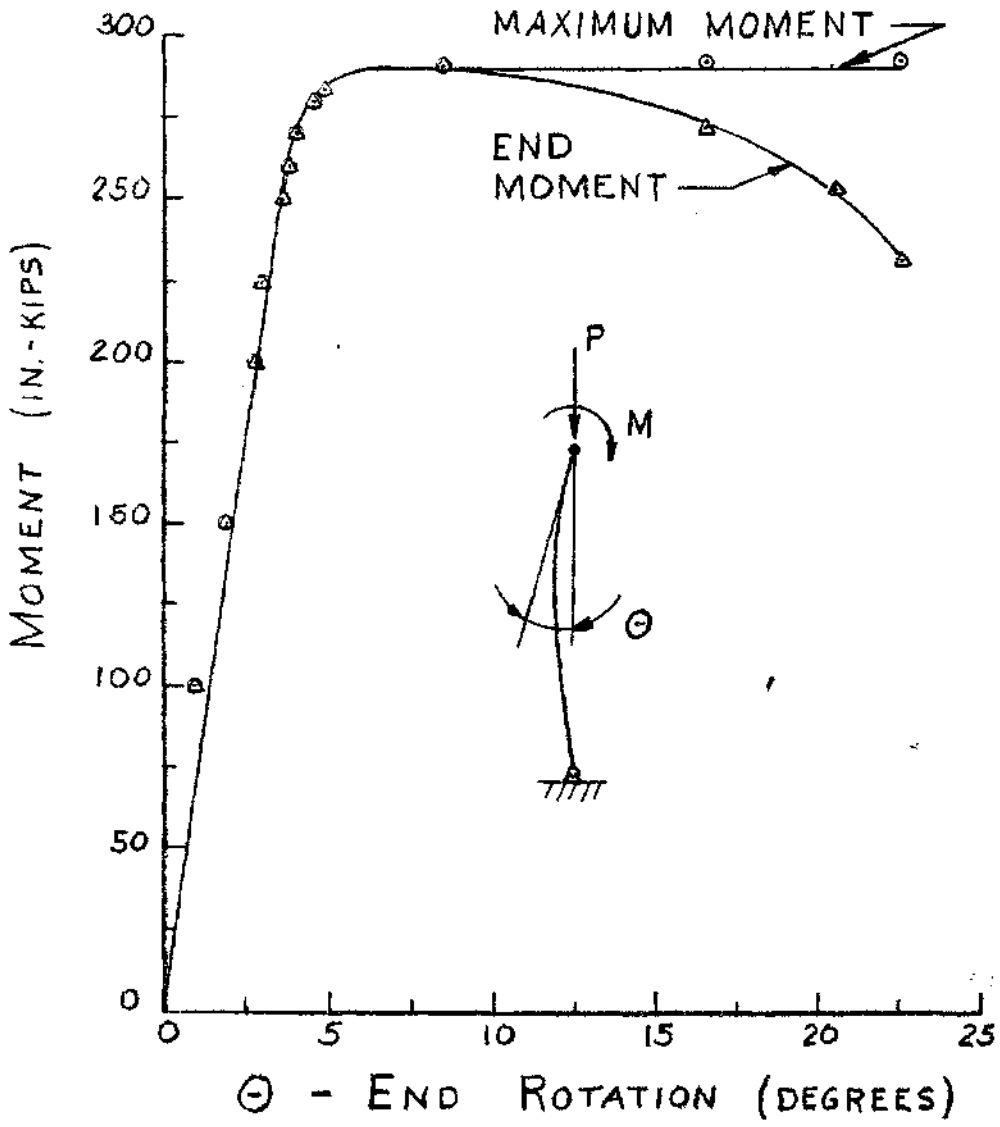

Figure 18. Test 1 : Moment vs. End Rotation

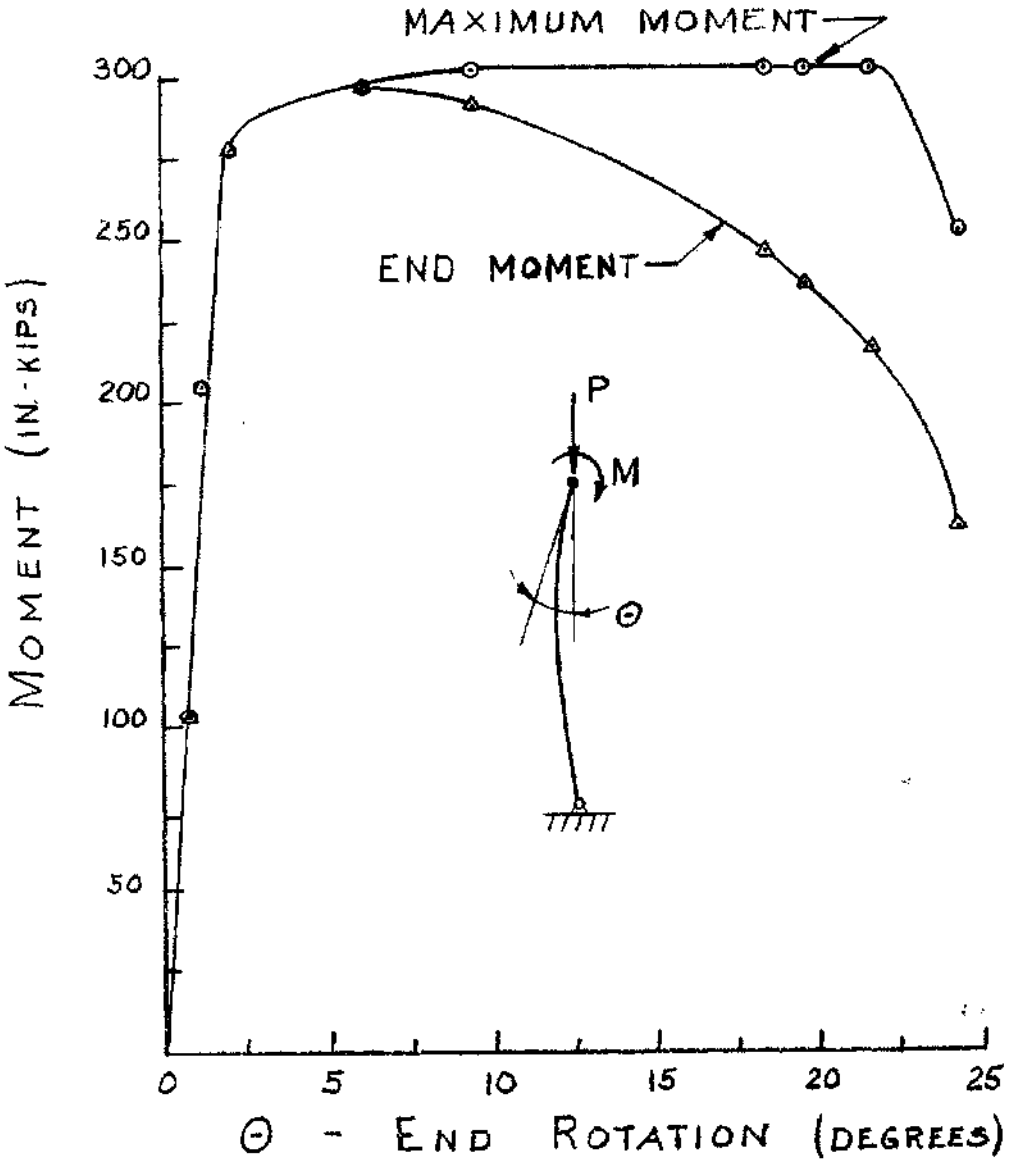

Figure 19. Test 2 : Moment vs. End Rotation

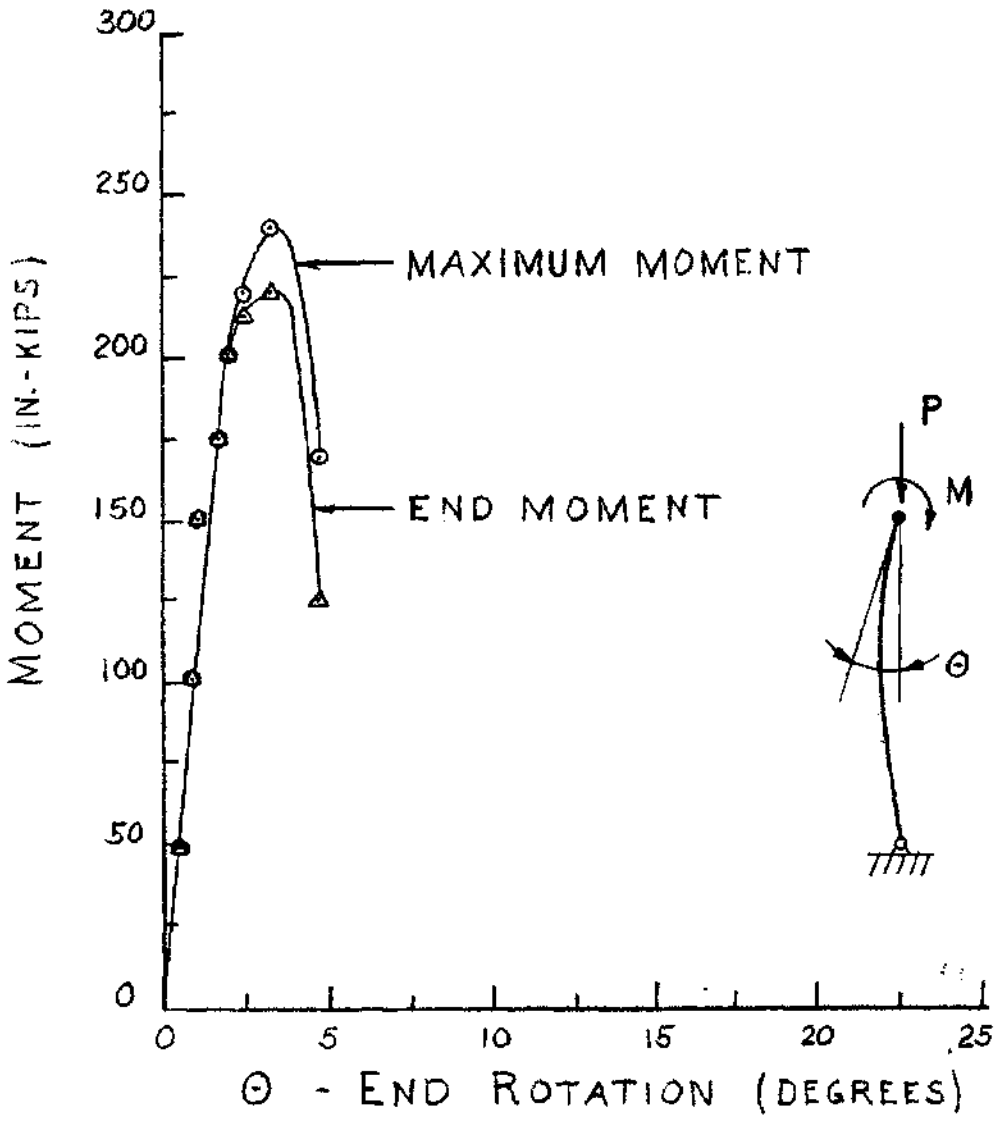

Figure 20. Test 3 : Moment vs. End Rotation

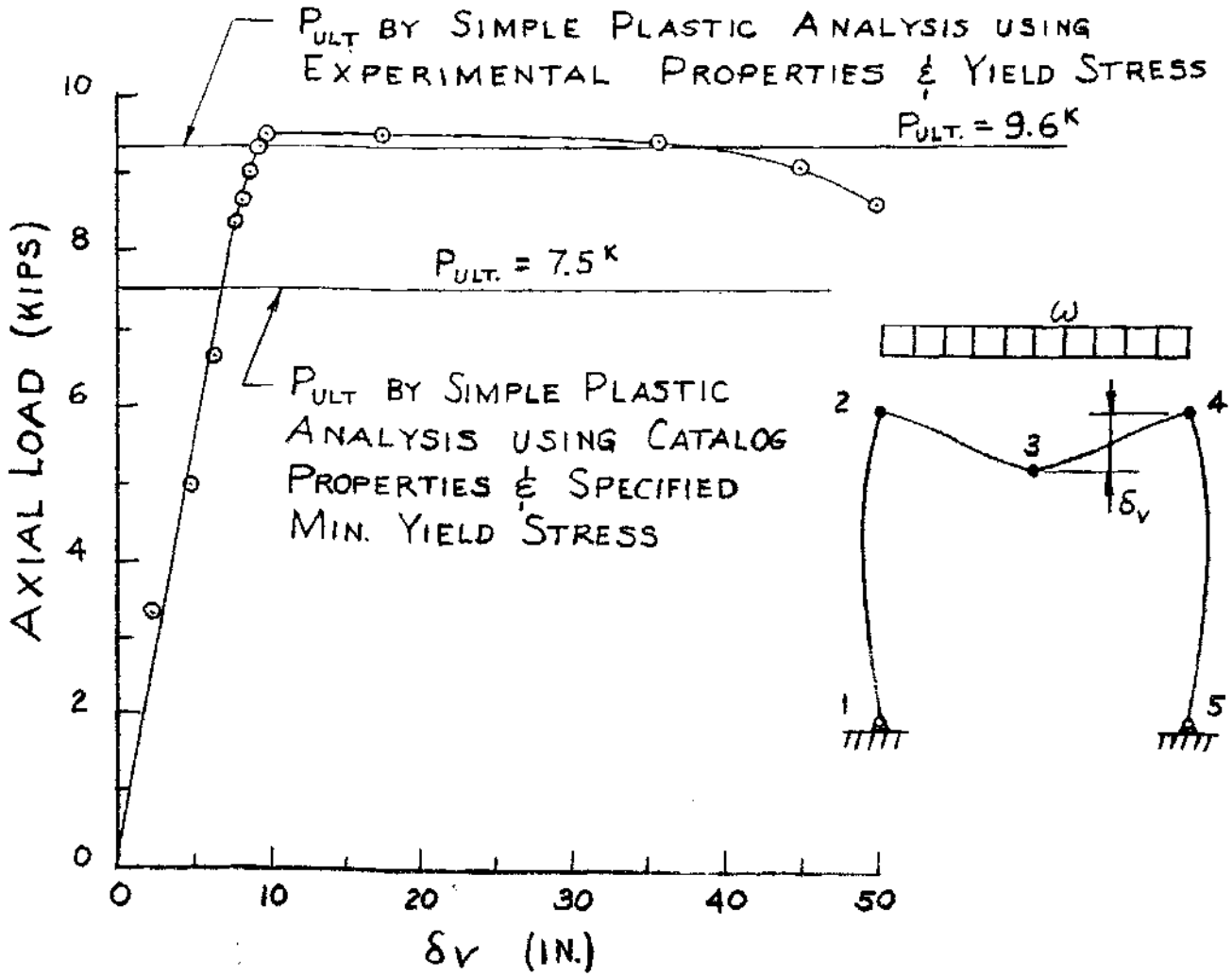

Figure 21. Test 1 : Axial Load vs. Midspan Deflection

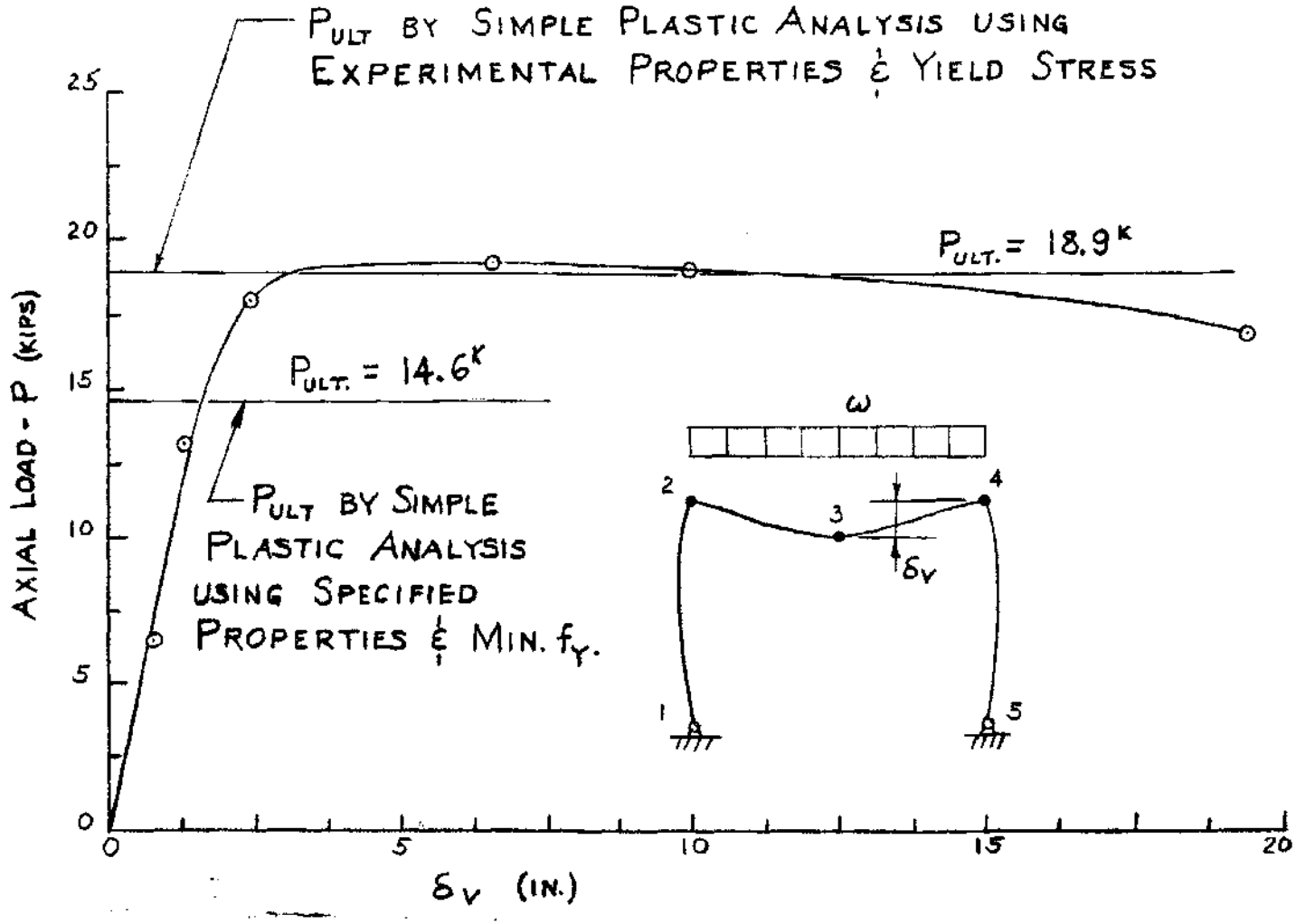

Figure 22. Test 2 : Axial Load vs. Midspan Deflection

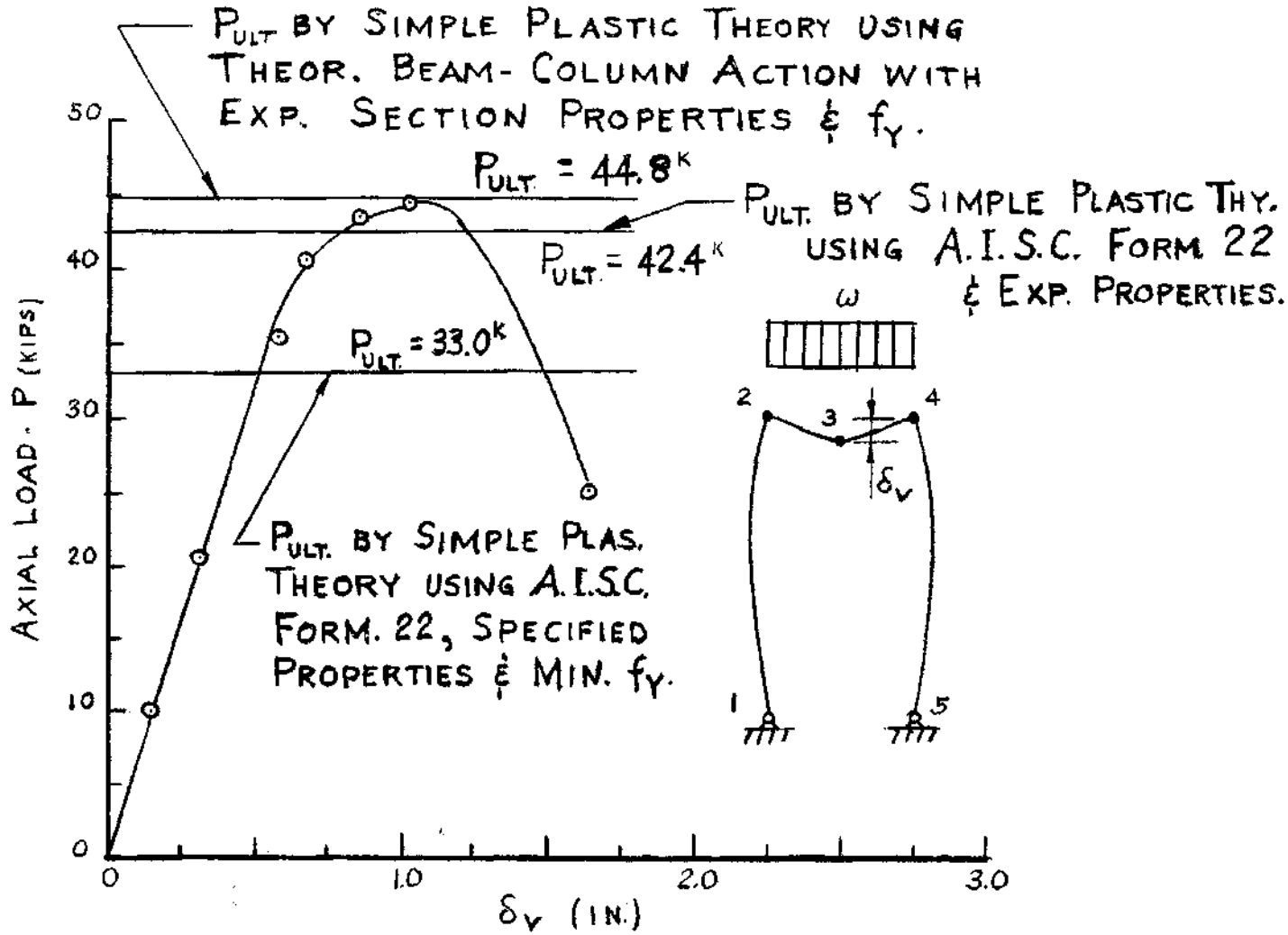

Figure 23. Test 3 : Axial Load vs. Midspan Deflection

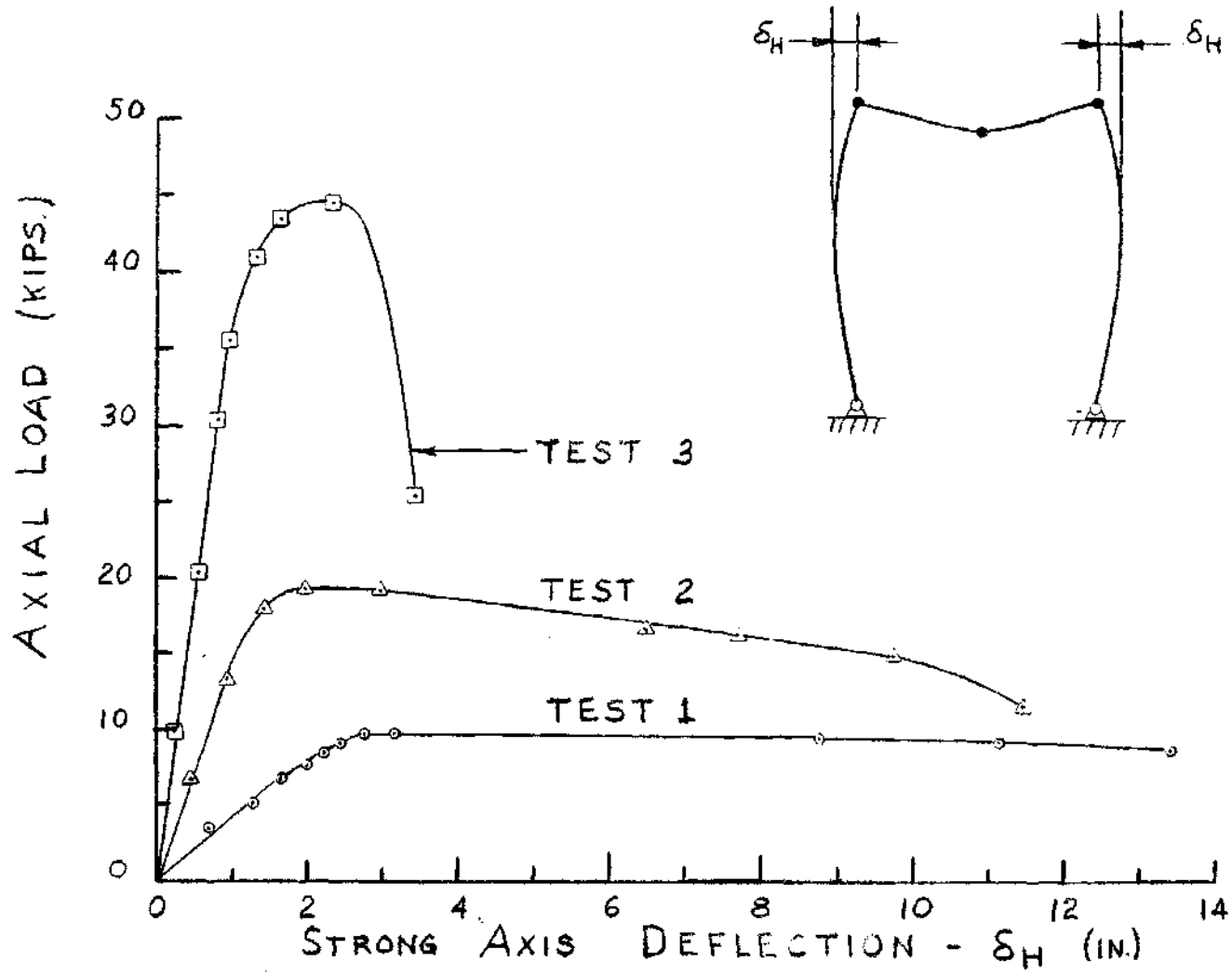

Figure 24. All Tests : Axial Load vs. Strong Axis Deflection

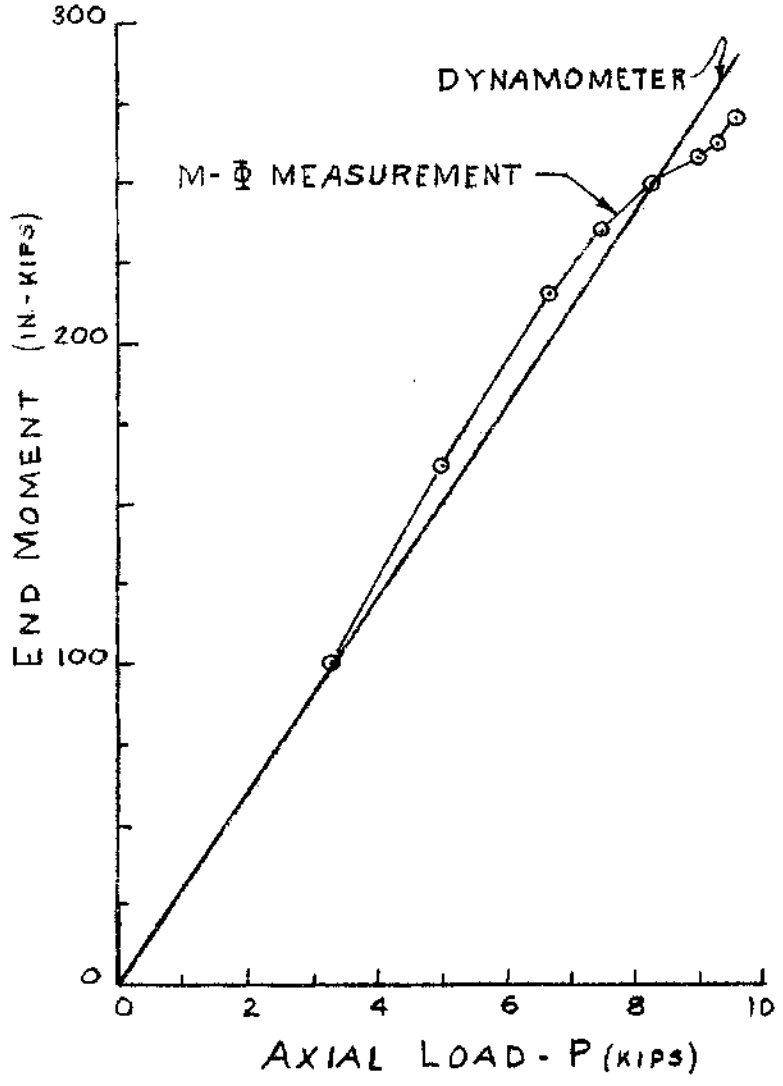

Figure 25. Test 1 : End Moment Correlation by Dynamometer and M - Φ Device

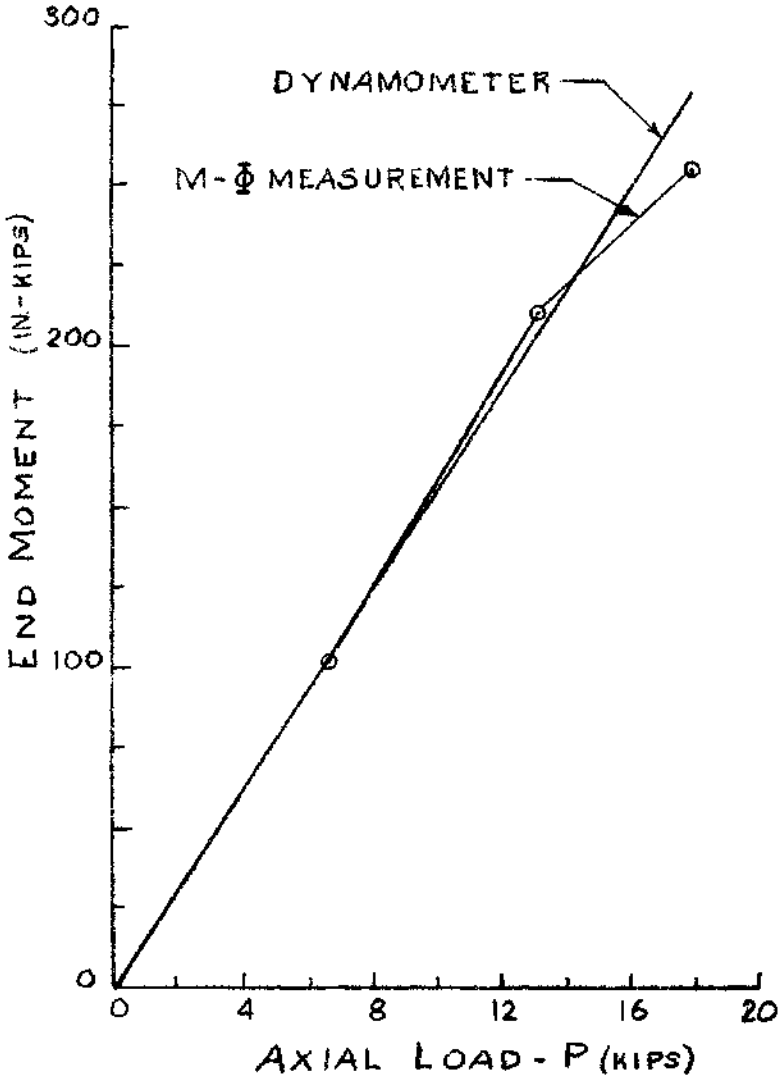

Figure 26. Test 2 : End Moment Correlation
by Dynamometer and M - Φ Device

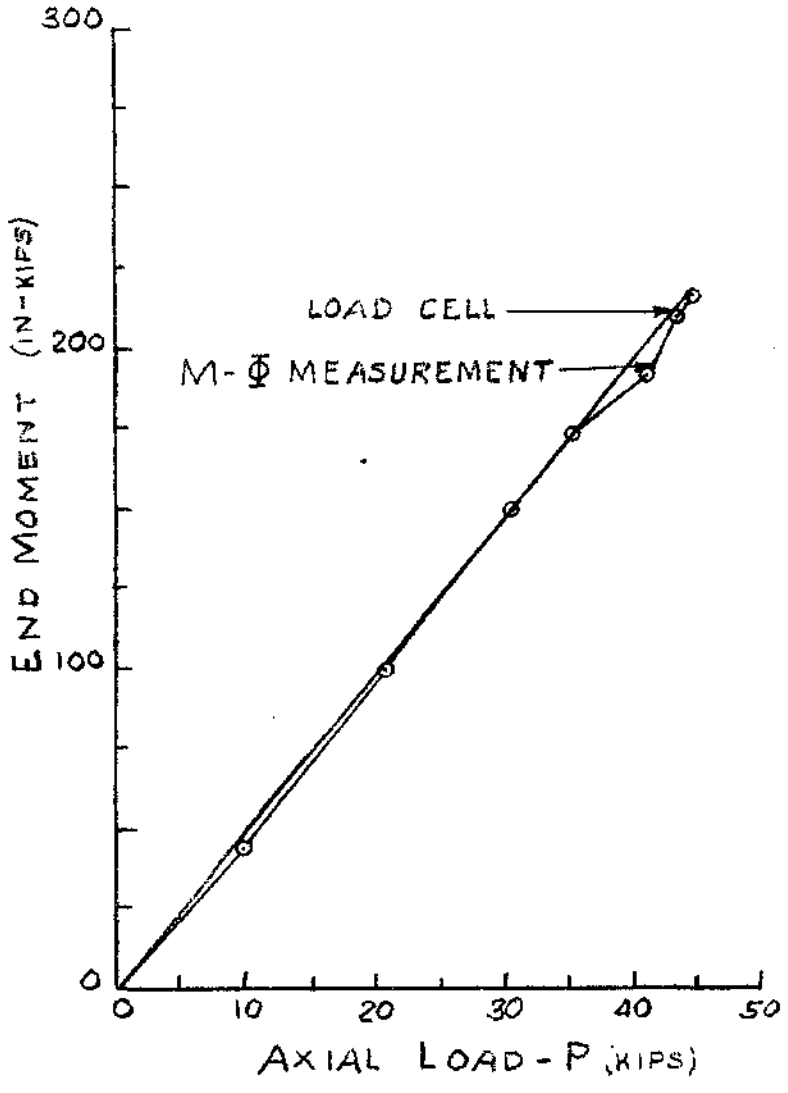

Figure 27. Test 3 : End Moment Correlation by Load Cell and M - Φ Device

APPENDIX C

TABLES

Table 1. M - Φ Test Results

— Pure Moment Beam Test —

①	②	③	④	⑤	①	②	③	④	⑤
READING	$\Sigma\Delta$ ($\times 10^{-3}$ IN.)	ϵ_c ($\times 10^{-3}$ IN/IN)	Φ ($\times 10^{-3}$ RAD/IN)	M (IN-KIP)	READING	$\Sigma\Delta$ ($\times 10^{-3}$ IN.)	ϵ_c ($\times 10^{-3}$ IN/IN)	Φ ($\times 10^{-3}$ RAD/IN)	M (IN-KIP)
1	17.3	.360	.117	50	13	81.5	1.70	.563	240
2	33.0	.687	.231	100	14	83.7	1.74	.579	245
3	49.0	1.02	.343	150	15	87.0	1.81	.603	250
4	57.7	1.20	.406	175	16	92.0	1.91	.637	255
5	63.0	1.31	.437	188	17	95.5	1.99	.661	260
6	66.0	1.37	.457	200	18	98.7	2.05	.683	265
7	69.5	1.45	.482	210	19	105	2.19	.727	270
8	71.5	1.49	.495	215	20	110	2.29	.760	275
9	73.5	1.53	.509	220	21	117	2.43	.810	280
10	75.5	1.57	.523	225	22	186.5	3.88	1.29	285
11	77.7	1.62	.537	230	23	300.5	6.25	2.08	287
12	79.7	1.66	.552	235					

Table 2. Coupon Test Results

①	②	③	④	⑤	⑥	⑦	⑧	⑨
COUPON NUMBER	WIDTH	t	A (IN^2)	P_Y (KIPS)	f_Y (ksi.)	$P_{ULT.}$ (KIPS)	$f_{ULT.}$ (ksi.)	% ELONGATION
1	.469"	.182"	.0855	3.700	43.4	5.66	66.2	26.5
2	.4835	.1812"	.0877	3.812	43.4	10.05	114.8	28.5
3	.4835	.1812"	.0877	3.900	44.5	5.625	64.2	30.0
AVERAGE RESULTS	—	—	—	—	43.8	—	65.2	28.3

Table 3. Micrometer Measurement of Wall Thickness

①	②	③	④	⑤
READING	FLANGE THICKNESS		WEB THICKNESS	
	TOP (IN.)	BOTT. (IN.)	LT. (IN.)	RT. (IN.)
1	.188	.182	.185	.183
2	.186	.178	.181	.180
3	.189	.181	.178	.180
4	.187	.188	.174	.187
5	.190	.192	.168	.189
6	—	—	.169	.189
7	—	—	.180	.191
AVERAGE THICKNESS	.1857"		.1812"	

Table 4. Experimentally Determined Section Properties

①	②	③
	SPECIFIED PROPERTY	EXP. PROPERTY
DEPTH - d (IN.)	6.000	6.030
WIDTH - w (IN.)	3.000	3.043
FLANGE THICKNESS - t_F (IN.)	.1875	.1857
WEB THICKNESS - t_w (IN.)	.1875	.1812
AREA - A ($IN.^2$)	3.113	3.175
YIELD LOAD P_Y (KIPS)	112.0	139.2
ULT. LOAD P_{ULT} (KIPS)	—	207.2
YIELD MOMENT M_Y (IN.-KIPS)	168	219.5
ULT. MOMENT M_p (IN.-KIPS)	225	292
I_{xx} (IN^4)	13.99	15.11
I_{yy} (IN^4)	4.755	5.13
r_{xx} (IN.)	2.12	2.18
r_{xx} (IN.)	1.24	1.27
Φ_{ELAS} (RAD.)	—	.00778

Table 5. Required Plastic Rotation - Midspan Hinge

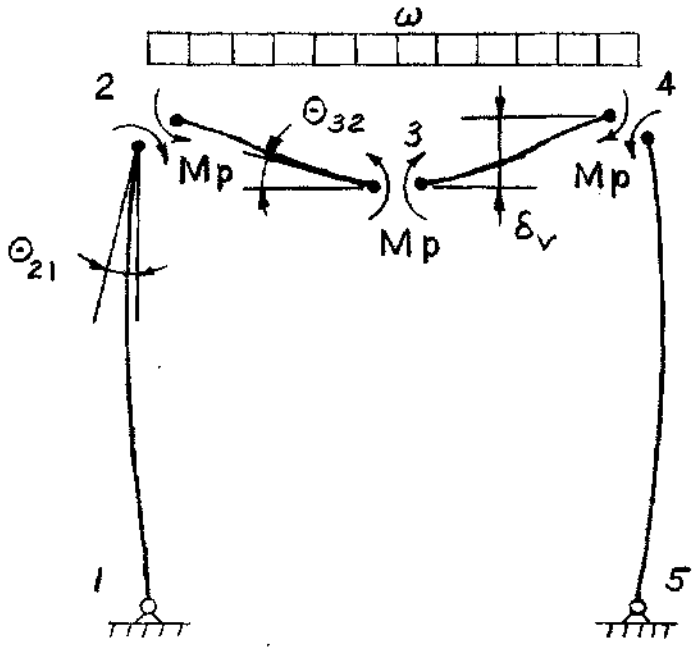

	Θ_{21} RAD.	δ_v IN.	Θ_{32} RAD.	% ELASTIC ROTATION
FRAME 1 252" x 240"	.0547	6.68	.0291	374 %
FRAME 2 172" x 120"	.0374	2.27	.0246	316 %
FRAME 3 172" x 40"	.0555	1.080	.0542	695 %

SLOPE DEFLECTION EQUATION:

$$\Theta_{AB} = \Theta'_{AB} + \delta/L + L(M_{AB} - M_{BA}/2)/3EI$$

Table 6. Test 1 - Summary of Data

(1)	(2)	(3)	(4)	(5)	(6)	(7)	(8)	(9)	(10)
READING	AXIAL LOAD (KIPS)	END MOM. (IN.-KIP)	MAX. MOM. (IN.-KIP)	MAX. TWIST ($\times 10^{-3}$ RAD)	MAX. LAT. DEFL. (IN.)	δ_H (IN.)	$\odot$ (DEGREES)	Φ ($\times 10^{-3}$ RAD/IN.)	δ_V (IN.)
1	0.00	0	0	0.00	0.00	0.00	0.00	0.00	0.00
2	3.33	100	100	0.00	0.03	0.79	0.95	.201	2.16
3	5.00	150	150	0.00	0.04	1.25	1.95	.328	4.85
4	6.67	200	200	0.00	0.04	1.72	2.76	.446	6.27
5	7.50	225	225	0.88	0.05	1.98	2.95	.504	6.56
6	8.30	250	250	0.00	0.06	2.20	3.54	.588	7.66
7	8.67	260	260	-1.17	0.06	2.32	3.75	.630	8.05
8	9.02	270	270	-1.46	0.07	2.42	4.00	.722	8.54
9	9.33	280	280	-2.92	0.08	2.57	4.50	.815	9.38
10	9.52	285	285	-2.92	0.09	2.65	4.70	.924	9.75
11	9.52	288	290	-1.75	0.10	2.73	4.75	1.22	9.83
12	9.51	286	292	-3.79	0.17	3.14	8.30	4.06	17.4
13	9.46	274	291	-5.53	1.18	8.79	16.5	4.20	35.5
14	9.11	256	292	-8.73	2.03	11.15	20.7	4.20	44.7
15	8.63	238	290	-16.1	2.75	13.40	22.5	4.20	49.7

Table 7. Test 2 - Summary of Data

(1)	(2)	(3)	(4)	(5)	(6)	(7)	(8)	(9)	(10)
READING	AXIAL LOAD (KIPS)	END MOM. (IN.-KIPS)	MAX. MOM. (IN-KIPS)	MAX. TWIST ($\times 10^{-3}$ RAD)	MAX. LAT. DEFL. (IN.)	δ_H (IN.)	Θ (DEGREES)	Φ ($\times 10^{-3}$ RAD/IN.)	δ_V (IN.)
1	0.00	0	0	0.00	0.00	0.00	0.00	0.00	0.00
2	6.64	103	103	0.00	0.01	0.45	0.78	.201	0.77
3	13.2	205	205	1.75	0.00	0.93	1.18	.437	1.29
4	18.0	278	278	1.45	0.08	1.40	2.14	.765	2.39
5	19.2	297	297	-1.45	0.12	1.98	6.05	5.46	6.54
6	19.1	291	304	-2.90	0.24	2.95	9.40	6.85	10.0
7	16.8	247	304	+3.20	1.10	6.47	18.4	6.80	19.4
8	16.2	236	304	+11.3	1.60	7.70	19.7	6.78	20.7
9	15.0	216	304	+17.5	2.68	9.75	21.7	6.73	22.8
10	11.5	162	252	+45.2	5.02	11.5	24.3	6.59	25.5

Table 8. Test 3 - Summary of Data

1	2	3	4	5	6	7	8	9	10
READING	AXIAL LOAD (KIPS)	END MOM. (IN-KIPS)	MAX. MOM. (IN-KIPS)	MAX. TWIST ($\times 10^{-3}$ RAD)	MAX. LAT. DEFL. (IN.)	δ_H (IN.)	Θ (DEGREES)	Φ ($\times 10^{-3}$ RAD/IN.)	δ_V (IN.)
1	0.00	0	0	0.00	0.00	0.00	0.00	0.00	0.00
2	9.93	49.0	49.0	0.00	0.00	0.22	0.42	0.11	0.14
3	20.4	101	101	1.17	0.02	0.55	0.87	0.25	0.30
4	30.3	150	150	5.24	0.06	0.80	1.04	0.37	0.35
5	35.3	175	175	8.18	0.11	0.95	1.70	0.45	0.58
6	40.7	201	201	8.18	0.12	1.30	1.97	0.57	0.68
7	43.2	213	220	0.87	0.29	1.60	2.46	0.73	0.85
8	44.4	220	240	4.37	1.05	2.30	3.28	0.85	1.14
9	25.2	125	168	25.0	3.95	3.40	4.75	0.92	1.64

Table 9. Test 3 - Comparison of Deflection & Moment Experimental & Theoretical

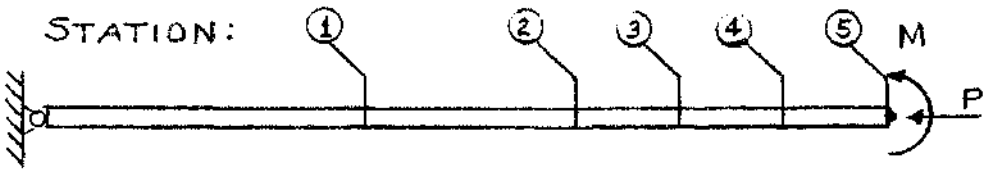

		STA. 1	STA. 2	STA. 3	STA. 4	STA. 5
STRONG AXIS DEFLECTION δ_H (IN.)	EXP.	1.76	—	1.96	1.19	0.00
	THEOR.	1.80	2.23	1.96	1.19	0.00
MOMENT M (IN.-KIP)	EXP.	153	—	240	237	220
	THEOR.	151	219	234	229	206

Table 10. Comparison of Test Results

	①	②	③	④	⑤	⑥	⑦	⑧
	SLENDERNESS RATIOS		AXIAL LOAD RATIOS			MOMENT RATIOS		END ROT.
	L/r_{xx}	L/r_{yy}	$\frac{P_{ULT.}}{P_Y}$	$\frac{P_{ULT.}}{P_{Cr}}$	$\frac{P_{ULT.}}{P_{24}}$	$\frac{M_o}{M_p}$	$\frac{M_{EXP.}}{M_p}$	Θ (DEGREES)
TEST 1	120	203	6.8%	45 %	32 %	1.0	1.0	22.5°
TEST 2	80	139	13.8%	42 %	31 %	.97	1.0	23.4°
TEST 3	80	139	31.9%	91 %	71 %	.72	.76	3.5°

BIBLIOGRAPHY

REFERENCES

1. Manual of Steel Construction, Sixth Edition, New York, New York: American Institute of Steel Construction, 1965, pp. 5-51 - 5-55.

2. Galambos, T. V., Inelastic Lateral-Torsional Buckling of Eccentrically Loaded Wide-Flange Columns, Ph. D. Dissertation, Lehigh University, 1959.

3. Metals Test Methods, 1958 Book of A. S. T. M. Standards, Part 3, Philadelphia 3, Pennsylvania: A. S. T. M., 1958.

4. Commentary On Plastic Design In Steel, New York, New York: Welding Research Council and The American Society of Civil Engineers, 1961.

5. Ketter, R. L. and Kaminsky, E. L., "Plastic Deformation of Wide-Flange Beam-Columns", Transactions, A. S. C. E., Vol. 1, Part 1, 1955, pp. 1028 - 1060.

6. Ketter, R. L. and Galambos, T. V., "Columns Under Combined Bending and Thrust", Transactions, A. S. C. E., Vol. 126, Part 1, 1961, pp. 1 - 25.

7. Newmark, N. M., "Numerical Procedure for Computing Deflections, Moments, and Buckling Loads", Transactions, A. S. C. E., Vol. 108, 1943, pp. 1161 - 1188.

OTHER LITERATURE

1. Moran, R., Lateral Stability of Box Beams Subject to Plastic Moment, Unpublished M. S. Thesis, Georgia Institute of Technology, 1958.

2. Ketter, R. L., "Further Studies of the Strength of Beam-Columns", Journal of the Structural Division, Proceedings, A. S. C. E., Vol. 87, 1961.

3. Estuar, F. R. and Tall, L., The Column Strength of Hot-Rolled Tubular Shapes -- An Experimental Evaluation, Fritz Engineering Laboratory Report No. 296.1, Lehigh University, Bethlehem, Pennsylvania, 1965.